Heliyon 10 (2024) e26920

Contents lists available at ScienceDirect

Heliyon

journal homepage: www.cell.com/heliyon

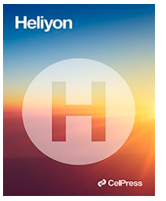

Research article

NADPH oxidase-mediated reactive oxygen species, antioxidant isozymes, and redox homeostasis regulate salt sensitivity in maize genotypes

Md. Motiar Rohman [a,**], Md. Robyul Islam [b], Sheikh Hasna Habib [c], Dilwar Ahmed Choudhury [d], Mohammed Mohi-Ud-Din [e,*]

[a] Plant Breeding Division, Bangladesh Agricultural Research Institute, Gazipur 1701, Bangladesh
[b] SAARC Agriculture Centre, Bangladesh Agricultural Research Council, Dhaka 1215, Bangladesh
[c] Oil Seed Research Centre, Bangladesh Agricultural Research Institute, Gazipur 1701, Bangladesh
[d] Agronomy Division, Bangladesh Agricultural Research Institute, Gazipur 1701, Bangladesh
[e] Department of Crop Botany, Bangabandhu Sheikh Mujibur Rahman Agricultural University, Gazipur 1706, Bangladesh

ARTICLE INFO

Keywords:
Ion homeostasis
Maize
NOX
Oxidative stress
Relationship
Salinity

ABSTRACT

The aim of the study is to examine the relationship between oxidative bursts, their regulation with ion homeostasis, and NADPH oxidase (NOX) in different salt-sensitive maize genotypes. For this, in the first study, four differently salt-sensitive maize genotypes (BIL214 × BIL218 as tolerant, BHM-5 as sensitive, and BHM-7 and BHM-9 as moderate-tolerant) were selected on the basis of phenotype, histochemical detection of reactive oxygen species (ROS), malondialdehyde (MDA) content, and specific and in-gel activity of NOX. In the next experiment, these genotypes were further examined in 200 mM NaCl solution in half-strength Hoagland media for nine days to study salt-induced changes in NOX activity, ROS accumulation, ion and redox homeostasis, the activity of antioxidants and their isozyme responses, and to find out potential relationships among the traits. Methylglyoxal (MG) and glyoxalse enzymes (Gly I and II) were also evaluated. Fully expanded leaf samplings were collected at 0 (control), 3, 6, 9-day, and after 7 days of recovery to assay different parameters. Na^+/K^+, NOX, ROS, and MDA contents increased significantly with the progression of stress duration in all maize genotypes, with a significantly higher value in BHM-5 as compared to tolerant and moderate-tolerant genotypes. A continual induction of Cu/Zn-SOD was observed in BIL214 × BIL218 due to salt stress. Substantial decreases in CAT2 and CAT3 isozymes in BHM-5 might be critical for the highest H_2O_2 burst in that sensitive genotype under salt stress. The highest intensified POD isozymes were visualized in BHM-5, BHM-7, and BHM-9, whereas BIL214 × BIL218 showed a continual induction of POD isozymes, although GPX activity decreased in all the genotypes at 9 days. Under salt stress, the tolerant genotype BIL214 × BIL218 showed superior ASA- and GSH-redox homeostasis by keeping GR and MDHAR activity high. This genotype also had a stronger MG detoxification system by having higher glyoxalase activity. Correlation, comparative heatmap, and PCA analyses revealed positive correlations among Na^+/K^+, NOX, $O_2^{\bullet-}$, H_2O_2, MG, proline, GR, GST, and Gly I activities. Importantly, the relationship depends on the salt sensitivity of the genotypes. The reduced CAT activity as well as redox homeostasis were critical to the survival of the sensitive genotype.

* Corresponding author.
** Corresponding author.
E-mail addresses: mrahman@bari.gov.bd (Md.M. Rohman), mmu074@bsmrau.edu.bd (M. Mohi-Ud-Din).

https://doi.org/10.1016/j.heliyon.2024.e26920
Received 20 October 2023; Received in revised form 14 February 2024; Accepted 21 February 2024
Available online 26 February 2024

1. Introduction

Salinity is a serious problem for the productivity of crops and diversity globally, threatening agricultural food production and food safety [1,2]. Alarmingly, over half of the world's population (52% or 4.03 billion individuals) in 13 countries resides in regions affected by salinity [3], and this number could surpass 5 billion by 2050 [4]. A recent survey reveals that approximately 1125 million hectares of terrestrial land are presently afflicted by salinity [5], and this acreage is expanding at an astonishing rate of approximately 2–3 ha per minute [6]. Furthermore, the economic losses due to salinity in crop production have exceeded USD 27.3 billion [7] and continue to rise, as agriculture worldwide heavily relies on irrigation, leading to increased salt content in irrigation water [3].

Under salt-stress conditions, plants suffer from damage to their photosynthetic machinery, primarily through impaired stomatal regulation and the accumulation of toxic levels of Na^+ ions in the cytosol [2]. Consequently, plants experience an excess of absorbed light for photosynthesis, leading to the generation of reactive oxygen species (ROS) in chloroplasts, resulting in oxidative stress [8]. The excessive accumulation of ROS, including H_2O_2, superoxide ($O_2^{\bullet-}$), and hydroxyl radicals ($HO^{\bullet}$) [9], severely disrupts plant metabolism and cell viability. In the most severe cases, this can trigger lipid peroxidation in cell membranes, DNA damage, protein denaturation, carbohydrate oxidation, pigment breakdown, and impaired enzymatic activity [9–12].

To counteract the detrimental effects of salt-induced stress, it is essential to understand the complex mechanisms involving multiple sub-traits, such as ion homeostasis, osmotic balance, and oxidative stress tolerance, each with a complex genetic basis [13]. These mechanisms are orchestrated by a highly intricate network of interconnected signaling pathways, including those related to ROS and nitrogen (NO) species [14–16], hormones [17,18], polyamines [19], phospholipids [20], and inorganic ions like free cytosolic Ca^{2+} [21,22] and K^+ [23,24]. Consequently, genetic engineering for salt-tolerant crops remains a significant challenge [25,26]. Moreover, breeding crops for Na^+ exclusion has limited potential for sustainable agricultural production [3], and the energy cost of adaptation is substantial [27]. To produce salt-tolerant crops, we need to change our perspective and focus on traits that were ignored during the domestication of staple crops. These traits include keeping redox balance and signaling ROS mechanisms effectively, which are common in salt-tolerant plants [28].

One of the pivotal players in universal ROS signaling is nicotine adenine dinucleotide phosphate (NADPH) oxidase, though some other class III peroxidases and specific cell wall oxidases are also involved in signaling [29–32]. NADPH oxidase (NOX), belonging to the NOX family, is an enzyme complex situated in the plasma membrane [33,34] that produces extracellular $O_2^{\bullet-}$ when activated [33]. Salt stress triggers NOX activation, both at the transcriptional and functional levels [35–37], and establishes a well-organized and self-amplifying mechanism known as the "ROS-Ca^{2+} hub" [31,33,38,39]. This mechanism can enhance the extent and amplitude of weak signals and translate them into a wide range of responses. As a result, transcriptional changes occur in the expression levels of key genes [40–42] due to alterations in the activity [43] and intracellular distribution of crucial membrane transporters [44]. This mechanism also enables long-distance systemic signaling between roots and shoots [30,45]. Notably, this self-amplification mechanism is distinct from other major ROS sources (e.g., chloroplasts, mitochondria, or peroxisomes), which makes NOX unique for stress-induced ROS signaling in plants. Although significant knowledge has been achieved, the relationship between NOX and ROS regulation needs more study to gain insight into their regulation, particularly in salt stress.

The impact of salt stress on antioxidant defense and redox regulation has been extensively studied in crops like wheat seedlings (*Triticum durum* Desf.). NADPH oxidase plays a role in the production of ROS in response to nickel-induced oxidative stress [46]. NADPH oxidase-mediated H_2O_2 production is also an intermediary step in the NaCl-induced elevation of calcium (Ca) levels in wheat roots [47]. In *Arabidopsis*, *AtrbohD* and *AtrbohF*, encoding NADPH oxidases, contribute to ROS production, regulating Na^+/K^+ homeostasis and enhancing salt tolerance in *Arabidopsis* seedlings [37,48]. The impact of NOX, along with the heavy metal chelator EDTA, and ROS scavengers on maize seed germination and seedling growth were examined under Pb stress [49]. In wheat, salinity reduced the activities of SOD, CAT, GR, MDHAR, and DHAR, while nitrogen supplementation increased SOD activity by 2-fold and APX activity by 3-fold compared to untreated plants [50]. Parvin et al. [51] investigated the effects of salinity and the ameliorative effect of vanillic acid on the antioxidant system in *Solanum lycopersicum*, demonstrating that salt stress decreased the activity of ASA/DHA, GSH/GSSG, GST, SOD, and CAT while vanillic acid increased the activity of ASA/DHA, GSH/GSSG, MDHAR, GR, GST, SOD, and CAT. However, most of these studies focused solely on the total activities of enzymatic antioxidants and generated data during specific periods after stress imposition, failing to assess changes in their isoenzyme patterns, which are also crucial for plant cell adaptation to shifts in the cellular redox environment. Nonetheless, the roles of ROS in signaling, especially those mediated by NADPH oxidases in maize, are still largely unexplored, especially during specific periods of salt stress. For instance, Rodríguez et al. [52] investigated the relationship between NOX, $O_2^{\bullet-}$, and the activities of SOD, peroxidase, and ascorbate in the elongation zone of maize leaf segments subjected to step-wise NaCl treatments. Furthermore, similar relationships among NOX activity, K^+ levels, and H_2O_2/NO signaling have been studied in rice by Wang et al. [53] and Ijaz et al. [54]. Additionally, the role of H_2O_2 signaling has been examined in cucumber by Kabała et al. [55], and alkalization-mediated signaling has been explored in *Arabidopsis* by Sun et al. [56]. However, all of the studies considered only a few of the parameters. A comprehensive study with all the parameters might provide valuable insights into the cellular oxidative stress management under salinity. Therefore, it is imperative to elucidate changes in the isoenzyme patterns of antioxidant enzymes and glyoxalases associated with NOX activity in crops like maize, a C_4 crop with wide adaptability to adverse environments, to understand the salt-tolerant mechanism for its improvement.

Though some recent studies have highlighted the extensive damage suffered by maize under abiotic stresses, especially excessive salt or water deficit stress [57–61], investigations into NOX activity in maize under salinity stress, particularly in differently salt-sensitive maize genotypes and their isozyme responses, have been limited. Considering these, the experiment was designed to study the changes in NOX, ROS, activities of antioxidant enzymes and their isozyme responses, methylglyoxal detoxification system,

and ion and redox homeostasis at different days after the induction of salt stress; and to elucidate their relationship in salt-tolerant and -sensitive maize genotypes. In our experiment, maize seedlings were exposed to 200 mM NaCl-induced salinity and recorded data at 0, 3, 6, and 9 days of stress treatment. We also examined recovery data to gain a deeper understanding of the potential relationships among Na^+/K^+ levels, NOX activity, ROS, antioxidant isozymes, the glyoxalase system, and redox homeostasis in the maize genotypes.

2. Materials and methods

2.1. Plant materials and stress treatment

Fifty maize genotypes were grown on crusted rock media (perlite) for seven days after germination. Seven-day-old seedlings were then transferred to a hydroponic system and allowed to grow for an additional three days to recover from transplanting shock. For salinity screening, 150 mM NaCl was added to a half-strength Hoagland nutrient solution and maintained for one month. Four maize genotypes were selected on the basis of distinct phenotypic differences: BIL214 × BIL218 as salt-tolerant, BARI hybrid maize-5 (BHM-5) as sensitive, and BARI hybrid maize-7 (BHM-7) and BARI hybrid maize-9 (BHM-9) as moderate-tolerant (Fig. 1). These genotypes were further evaluated using histochemical detection of H_2O_2 and $O_2^{\bullet-}$ in leaf, MDA content, and NOX activity (specific and in-gel) to corroborate the phenotypic variability (Fig. S1).

We then studied the selected genotypes to investigate the relationship between salinity, NOX, ROS, enzymatic and non-enzymatic antioxidants, and related metabolites. After 3 days transplanting shock, the seedlings of the selected genotypes were exposed to a 200 mM NaCl solution in half-strength Hoagland media. This condition was maintained for nine days, followed by a seven-day recovery period in saline-free Hoagland media. Fully expanded leaf samples (8 cm from distal end) were collected at 0 (control), 3, 6, and 9 days after salinity stress for various parameters. Recovery data (R) were collected after seven days of salinity stress removal.

2.2. Protein extraction and quantification

Protein extraction followed the method described by Rohman et al. [57]. Leaf tissue (0.5 g) was homogenized in1ml 50 mM ice-cold K–P buffer (pH 7.0) containing 100 mM KCl, 1 mM ascorbate, 5 mM β-mercaptoethanol and 10% (w/v) glycerol. The centrifugation of homogenates was done at 11,500×*g* for 10 min at 0–4 °C, and the supernatants were used to assay enzyme activity. Protein quantification was performed spectrophotometrically using the Bradford et al. [62] method using BSA as standard.

2.3. Measurement of Na^+/K^+

Sodium (Na^+) and potassium (K^+) contents were assessed by extracting sap from freshly harvested roots and shoots using a tissue sap extractor (Horiba, Japan). Na^+ and K^+ contents were determined using compact Na^+ ion (Horiba-731, Japan) and K^+ ion (Horiba-722, Japan) meters, respectively, following Rohman et al. [60].

2.4. Assay of enzymatic activities

Activities of SOD (EC: 1.15.1.1), CAT (EC: 1.11.1.6), APX (EC: 1.11.1.11), POD (EC: 1.11.1.7), and GPX (EC: 1.11.1.9) activities were determined using the comprehensive methods described by Islam et al. [61]. SOD activity was assayed based on the xanthine-xanthine oxidase interaction. The reaction mixture contained K–P buffer (50 mM), nitroblue tetrazolium (NBT) (2.24 mM), xanthine oxidase (0.1 units), catalase (0.1 units), xanthine (2.36 mM), and enzyme extract. Catalase was added to avoid the H_2O_2-mediated possible inactivation of CuZn-SOD. The activity was expressed as units (amount of enzyme required to inhibit NBT reduction by 50%) min^{-1} mg^{-1} protein. For CAT activity, the reaction mixture contained 50 mM K–P buffer (pH 7.0), 15 mM H_2O_2, and

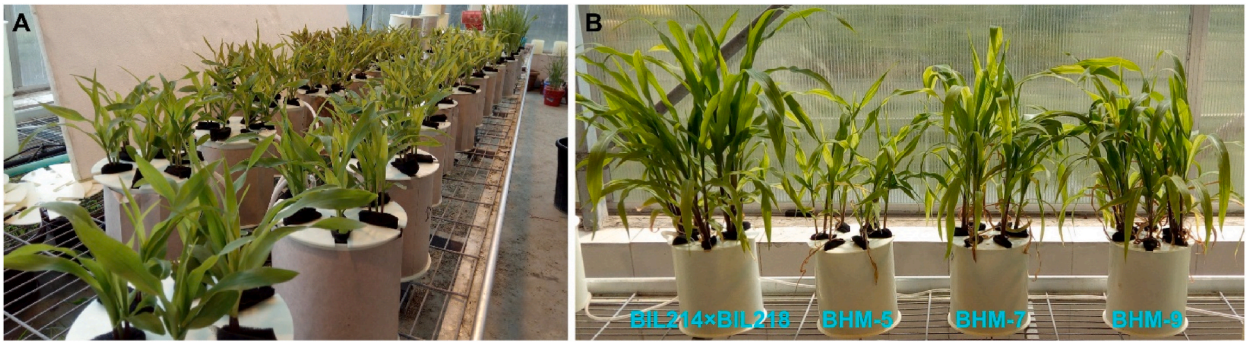

Fig. 1. Fifty maize genotypes in the screening block of the greenhouse (A) and comparative phenotypic difference of four selected maize genotypes during screening (B). Seven-day-old seedlings were then transferred to a hydroponic system and allowed to grow for an additional three days to recover from transplanting shock. For salinity screening, 150 mM NaCl was added to a half-strength and continued for 30 days.

enzyme solution in a final volume of 0.7 ml. The reaction was started with the addition of enzyme extract, and the activity was calculated using the extinction coefficient of 39.4 M^{-1} cm^{-1}. APX activity was assayed in a 0.7 ml reaction mixture containing 50 mM K–P buffer (pH 7.0), 0.50 mM ASA, 0.10 mM H_2O_2, 0.1 mM EDTA, and enzyme extract at 290 nm for 1 min. The activity calculated with an extinction coefficient of 2.8 $mM^{-1}cm^{-1}$. For POD activity, the reaction mixture contained 25 mM K–P buffer (pH 7.0), 0.05% guaiacol, 10 mM H_2O_2 and the enzyme extract, which was observed for 1 min at 470 nm for guaiacol oxidation. The activity was calculated using an extinction coefficient of 26.6 mM^{-1} cm^{-1}. APX activity was calculated with an extinction coefficient of 2.8 mM^{-1} cm^{-1}. The reaction mixture contained 50 mM K–P buffer (pH 7.0), 0.50 mM ASA, 0.10 mM H_2O_2, 0.1 mM EDTA, and enzyme solution. The absorbance changed was observed at 290 nm for 1 min. On the other hand, MDHAR (EC: 1.6.5.4), DHAR (EC: 1.8.5.1), GR (EC: 1.6.4.2), Gly I (EC: 4.4.1.5), and Gly II (EC: 3.1.2.6) activities were determined following the detailed procedures described in Monsur et al. [63]. One unit of SOD activity was defined as the protein amount needed to inhibit 50% of NBT. NOX (EC 1.6.3.1) activity was measured following the procedure of Jiang and Zhang [64]. The assay mixture contained 50 mM Tris-HCl buffer, pH 7.5, 0.5 mM XTT, 100 μM NADPH.Na_4, and 20 μg of protein. After the addition of NADPH, XTT reduction was monitored at 470 nm for 1 min. The adjustments of background production were determined in the presence of 50 U of SOD. Activity was calculated using the extinction coefficient, 2.16 × 104 $M^{-1}cm^{-1}$.

Non-denaturing polyacrylamide gel electrophoresis (PAGE) was used to separate equal amounts of protein, following the method of Laemmli [65]. SOD, CAT, POD, APX, GPX, and NOX isoenzymes were determined using the procedures described in Islam et al. [61]. NOX isoenzymes were detected by the NBT reduction method [66] with native PAGE using 8% gels, each well containing 50 μg of protein. The gels were stained in a solution containing 50 mM Tris-HCl buffer (pH 7.4), 0.2 mM NBT, 0.1 mM $MgCl_2$, and 1 mM $CaCl_2$ in the dark for 20 min. Subsequently, NADPH.Na_4 was added to the dye solution at a final concentration of 0.2 mM, and the appearance of blue formazan bands was observed. For Mn-SOD identification, at first, gels soaked in 8 mM H_2O_2 in 100 mM K–P buffer for 30 min at 75 rpm, ringed with DW, again soaked in 100 mM K–P buffer containing 28 mM riboflavin and 28 mM TEMED for 15 min again ringed with DW and then illuminate on a light box for at least 15 min for initiation of photochemical reaction. For Cu/Zn- and Fe-SOD identification, gels were soaked in 2 mm KCN and 0.04% H_2O_2. KCN inactivates Cu/Zn-SOD and H_2O_2 inactivates Fe-SOD. To inhibit both Cu/Zn-SOD and Fe-SOD, KCN and H_2O_2 were simultaneously used.

2.5. Assessment of the contents of superoxide ($O_2^{\bullet-}$), hydrogen peroxide (H_2O_2) and MDA

Radical superoxide ($O_2^{\bullet-}$) and hydrogen peroxide (H_2O_2) contents were determined in fully expanded maize leaves following the procedures of Elstner and Heupel [67] and Yu et al. [68], respectively. For $O_2^{\bullet-}$, leaves (0.3 g) were homogenized in 3 ml of 65 mM potassium-phosphate (K–P) buffer (pH 7.8) on an ice bath and centrifuged at 4 °C for 10 min at 5000×*g*. The supernatants (0.75 ml) were mixed with 0.675 ml of 65 mM K–P buffer (pH 7.8) and 0.07 ml of 10 mM hydroxylamine chlorhydrate and incubated at 25 °C. After 20 min, 0.375 ml of 17 mM sulfanilamide and 0.375 ml of 7 mM α-naphthylamine were added and incubated at 25 °C for another 20 min before it was mixed with 2.25 ml of diethyl ether. The absorbance was measured at 530 nm, and the $O_2^{\bullet-}$ concentration was calculated from a standard curve of $NaNO_2$. On the other hand, H_2O_2 was extracted by homogenizing 0.5 g of leaf samples with 3 ml of 50 mM K–P buffer (pH 6.5) at 4 °C and centrifuged at 11,500×*g* for 15 min. Three milliliters of the supernatant was mixed with 1 ml of 0.1% $TiCl_4$ in 20% H_2SO_4 (v/v) and stored in room temperature for 10 min and centrifuged at 11,500×*g* for 15 min. The optical absorption of the supernatant was measured spectrophotometrically at 410 nm to determine the H_2O_2 content and expressed as nmol g^{-1} fresh weight. The content of MDA (as lipid peroxidation) was determined according to Heath and Packer [69]. Concentration MDA was calculated with an extinction coefficient of 155 mM^{-1} cm^{-1} and expressed as nmol g^{-1} FW.

2.6. Histochemical ROS marker detection

Localization of $O_2^{\bullet-}$ and H_2O_2 in fully expanded maize leaves was tested following the procedures of Chen et al. [70] and Thordal-Christensen et al. [71], respectively. The leaves were stained in 0.1% NBT or 0.1% 3,3-diaminobenzidine (DAB) solution for 8 h under dark and light, respectively. Incubated leaves were then decolorized by immersing in boiling ethanol which allowed visualization of bluish insoluble formazan (for $O_2^{\bullet-}$) or deep brown polymerization product (for H_2O_2). After cooling, the sample was put in 95% ethanol until photograph taken.

2.7. Measurement of ascorbate, glutathione and proline contents

Maize leaves (0.5 g fresh weight) were homogenized in 3 ml ice-cold acidic extraction buffer containing 5% *meta*-phosphoric acid and 1 mM EDTA, and centrifuged at 4 °C for 15 min at 11,500×*g*, and the supernatant was used for the determination of glutathione (GSH), oxidized glutathione (GSSG), reduced ascorbate (ASA) and dehydroascorbate (DHA) contents as described in Rohman et al. [57]. Proline (Pro) contents were measured according to the protocol of Bates et al. [72].

2.8. Measurement of methylglyoxal (MG)

Methylglyoxal (MG) was measured following Rohman et al. [57]. Leaf tissue (0.3 g) was extracted in 3 ml of 0.5 M perchloric acid and ice incubation for 15 min, then centrifuged at 4 °C at 11,000×*g* for 10 min. The supernatant was decolorized by adding charcoal (10 mg ml^{-1}), kept for 15 min at room temperature, and then centrifuged at 11,000×*g* for 10 min at 20 °C. Before using the supernatant, it was neutralized by incubating for 15 min with saturated potassium carbonate solution at room temperature and centrifuged

again at 11,000×*g* for 10 min. Neutralized supernatant was used for MG estimation using N-acetyl-L-cysteine. The formation of the product N-α-acetyl-S-(1-hydroxy-2-oxo-prop-1-yl) cysteine was recorded at 288 nm wavelength.

2.9. Data analysis

Analysis of variance was done following factorial CRD design, where the individual effect of treatment and genotypes and their interaction were observed. Data obtained from the experiments were analyzed using statistical software Statistix-10. The means of treatment, genotypes, and interaction were compared using the least significant difference (LSD) test at a significant level of $p \leq 0.05$. Correlation plot was created with the R library corrplot [73]. R library pheatmap was adapted to generate heatmap and hierarchical clusters (distance = Euclidean and method = wardD2) [74]. PCA was performed with the libraries ggplot2, factoextra, and FactoMineR [75,76].

3. Results

3.1. Screening for salinity tolerance

A total of 50 maize genotypes were screened for salinity tolerance in the greenhouse (Fig. 1A). Four genotypes with clear phenotypic differences were selected for further study: BIL214 × BIL218 (tolerant), BHM-5 (sensitive), BHM-7, and BHM-9 (medium tolerance) (Fig. 1B). ROS ($O_2^{\bullet-}$ and H_2O_2) and MDA were used as selection criteria, and it was found that all concentrations were higher in the sensitive genotypes BHM-5 (Fig. S1). Histochemical detection of $O_2^{\bullet-}$ and H_2O_2 also supported these findings. Additionally, NOX activity, which plays a role in ROS production, was measured spectrophotometrically and by in-gel native activity, and it was significantly higher in BHM-5 (Fig. S1).

3.2. Regulation of ROS, NOX, antioxidants, and glyoxalase systems under salinity in selected maize genotypes

Analysis of variance (ANOVA) showed that treatment and genotype variances for all the studied traits were statistically significant (Table 1). The interaction between treatment and genotype was also significant for several traits, including NOX, K^+/Na^+, $O_2^{\bullet-}$, H_2O_2, CAT, POD, APX, GPX, MDHAR, DHAR, GR, Pro, MG, Gly I, and Gly II. This suggests that salt application has a significant impact on oxidative stress-related biochemical parameters and enzymatic activity.

3.3. Salt stress accelerated the Na^+/K^+ ratio, activity of NOX, and ROS generation

In comparison to the control condition, Na^+ accumulation increased exponentially in the maize plants due to salt supplementation,

Table 1
Analysis of variance showing mean squares for NOX (μmol min^{-1} mg^{-1} protein), Na^+/K^+ (ratio), superoxide ($O_2^{\bullet-}$; nmol g^{-1} FW min^{-1}), H_2O_2 (μmol g^{-1} FW), superoxide dismutase (SOD; Unit min^{-1} mg^{-1} protein), catalase (CAT; μmol min^{-1} mg^{-1} protein), peroxidase (POD; μmol min^{-1} mg^{-1} protein), ascorbate peroxidase (APX; μmol min^{-1} mg^{-1} protein), glutathione peroxidase (GPX; nmol min^{-1} mg^{-1} protein), monodehydroascorbate reductase (MDHAR; nmol min^{-1} mg^{-1} protein), dehydroascorbate reductase (DHAR; nmol min^{-1} mg^{-1} protein), glutathione reductase (GR; μmol min^{-1} mg^{-1} protein), GST (nmol min^{-1} mg^{-1} protein), ASA redox homeostasis [(ASA/(ASA + DHA)], GSH redox homeostasis [(GSH/(GSH + GSSG)], Proline (Pro; μmol g^{-1} FW), Methylglyoxal (MG; μmol g^{-1} FW), Gly I (μmol min^{-1} mg^{-1} protein), and Gly II (μmol min^{-1} mg^{-1} protein) of maize seedlings under salinity stress. * and ** means significant at $p \leq 0.05$, $p \leq 0.01$, respectively.

Source of variation	Treatment (T)	Genotype (G)	T × G	Error
df	4	3	12	80
NOX	4.27**	2.38**	0.53**	0.012
Na^+/K^+	19.7**	2.13**	0.459**	0.099
$O_2^{\bullet-}$	90.09**	56.29**	10.59**	0.312
H_2O_2	206.3**	81.2**	14.7**	0.39
SOD	1036.0**	404.5**	66.9*	35.7
CAT	477.1**	2549.5**	806.4**	20.7
POD	0.242**	0.163**	0.057**	0.006
APX	0.076**	0.063**	0.025**	0.007
GPX	2384.9**	1076.6**	513.9**	50.5
MDHAR	2075.7**	1713.5**	196.4**	59.1
DHAR	2681.0**	157.9**	470.2**	34.3
GR	4211.4**	320.7**	255.4**	36.7
GST	2886.3**	374.9**	146.5*	73.7
ASA/(ASA + DHA)	0.191**	0.043**	0.004*	0.002
GSH/(GSH + GSSG)	0.249**	0.022*	0.0014*	0.00075
Pro	79.47**	9.09**	1.46**	0.169
MG	2133.2**	340.3**	73.9**	6.12
Gly-I	1.09**	0.184**	0.030**	0.008
Gly-II	0.018**	0.005**	0.003**	0.001

while K^+ intake was drastically reduced. Consequently, the K^+/Na^+ ratio gradually decreased across the salt treatment. Specifically, on day 3 after salt imposition, the ratio decreased by 42, 50, 43, and 55% in the genotypes BIL214 × BIL218, BHM-5, BHM-7, and BHM-9, respectively, compared to their control. On day 6, the ratio decreased by 70, 82, 74, and 80% for the same sequence of genotypes. On day 9, K^+/Na^+ declined by 80, 93, 86, and 88% (Table 1). During the recovery treatment, the ratio significantly increased by 46. , 189142.1, and 76% in BIL214 × BIL218, BHM-5, BHM-7, and BHM-9 genotypes, respectively, compared to the individual 9th-day stress treatment (Table 1).

The activity of NOX increased in all the genotypes with the duration of salinity stress, with the content being consistently significantly higher in BHM-5 (Table 1). The highest activity of NOX was observed in BHM-5 on day 9. Compared to the control, NOX activity in the BHM-5 genotype increased by 147, 341, and 641% on days 3, 6, and 9 of salt imposition, respectively. In the BIL214 × BIL218 genotype, NOX activity increased by 68, 157, and 206% under salt stress on days 3, 6, and 9, respectively. In the case of BHM-7, NOX activity increased on days 3, 6, and 9 by 65, 130, and 186%, respectively. In BHM-9, NOX activity increased by 86, 147, and 233% on the 3rd, 6th, and 9th day of salinity imposition, respectively (Table 1). On day 9, the activity of NOX was 181, 153, and 156% higher in BHM-5 than in BIL214 × BIL218, BHM-7, and BHM-9, respectively. Conversely, during the recovery stage, salt stress-induced NOX activity decreased significantly in all the genotypes compared to their respective 9th day of stress treatment (Table 1). During screening, NOX activity was also higher in BHM-5 (Fig. S1), where two different NOX isozymes were detected. NOX1 was highly expressed in BHM-5 compared to BIL214 × BIL218, while NOX2 was found in all the treatments (Fig. S1).

3.4. Salinity stress increased both $O_2^{\bullet-}$ and H_2O_2 contents

Salinity stress led to an increase in both $O_2^{\bullet-}$ and H_2O_2 contents in the study. Superoxide ($O_2^{\bullet-}$) and H_2O_2 contents exhibited significant variations among treatments, genotypes, and their interactions (Table 1). These reactive oxygen species (ROS) levels increased in all genotypes as the duration of the induced stress progressed, with the highest increments observed in BHM-5 under stress conditions (Table 2). Specifically, in the BIL214 × BIL218 genotype, $O_2^{\bullet-}$ contents increased by 70, 130, and 191% on the 3rd, 6th, and 9th

Table 2
Effect of salinity stress on K^+/Na^+, Pro, $O_2^{\bullet-}$, and H_2O_2 in maize seedlings at different day intervals of stress treatments. Each value of data represents the mean of five replications ($n = 5$). Values within a column with different letters are significant at $p \leq 0.05$. Details are given in Table 1.

Source of Variation	Na^+/K^+	NOX	$O_2^{\bullet-}$	H_2O_2
Treatment				
Control (C)	0.248^{e}	0.39^{d}	2.02^{d}	2.20^{d}
Day 3 (3 d)	0.593^{d}	0.74^{c}	2.85^{c}	3.08^{c}
Day 6 (6 d)	1.41^{b}	1.13^{b}	5.17^{b}	7.24^{b}
Day 9 (9 d)	2.81^{a}	1.60^{a}	7.24^{a}	9.73^{a}
Recovery (R)	0.887^{c}	0.74^{c}	3.04^{c}	3.42^{c}
SE	0.099	0.04	0.18	0.20
F ratio (df = 4, 80)	198.9	346.3	289.0	517.2
Genotype				
BIL214 × BIL218	0.901^{c}	0.669^{c}	2.60^{c}	3.64^{c}
BHM-5	1.60^{a}	1.37^{a}	6.16^{a}	7.76^{a}
BHM-7	1.21^{b}	0.845^{b}	3.82^{b}	4.55^{b}
BHM-9	1.13^{b}	0.786^{b}	3.67^{b}	4.59^{b}
SE	0.198	0.031	0.158	0.179
F ratio (df = 3, 80)	21.5	192.8	180.6	203.7
Interaction				
C × BIL214 × BIL218	0.226^{g}	0.329^{j}	1.37^{m}	1.86^{j}
C × BHM-5	0.265^{g}	0.383^{j}	$2.50^{i\text{-}l}$	2.47^{ij}
C × BHM-7	0.257^{g}	0.450^{ij}	2.33^{jkl}	1.89^{j}
C × BHM-9	0.245^{g}	0.378^{j}	1.85^{lm}	$2.59^{h\text{-}j}$
3 d × BIL214 × BIL218	0.442^{g}	0.553^{hi}	$2.34^{j\text{-}l}$	2.71^{hi}
3 d × BHM-5	0.966^{ef}	0.946^{de}	$3.67^{e\text{-}g}$	3.86^{fg}
3 d × BHM-7	0.476^{g}	0.741^{fg}	$2.74^{h\text{-}k}$	2.53^{ij}
3 d × BHM-9	0.490^{g}	0.701^{g}	$2.67^{h\text{-}k}$	$3.22^{g\text{-}i}$
6 d × BIL214 × BIL218	1.01^{ef}	0.846^{ef}	$3.15^{g\text{-}i}$	4.28^{ef}
6 d × BHM-5	1.95^{d}	1.69^{b}	8.47^{b}	12.0^{b}
6 d × BHM-7	1.33^{e}	1.04^{d}	4.37^{de}	6.47^{d}
6 d × BHM-9	1.35^{e}	0.933^{de}	4.70^{d}	6.23^{d}
9 d × BIL214 × BIL218	1.93^{d}	1.01^{d}	$4.00^{d\text{-}f}$	6.86^{d}
9 d × BHM-5	3.71^{a}	2.84^{a}	12.50^{a}	15.54^{a}
9 d × BHM-7	3.04^{b}	1.29^{c}	6.32^{c}	8.53^{c}
9 d × BHM-9	2.55^{c}	1.26^{c}	6.13^{c}	7.97^{c}
R × BIL214 × BIL218	0.899^{f}	0.607^{gh}	2.13^{kl}	2.50^{ij}
R × BHM-5	1.12^{ef}	0.971^{de}	3.66^{fg}	4.93^{e}
R × BHM-7	0.957^{ef}	0.710^{fg}	$3.33^{f\text{-}h}$	3.33^{gh}
R × BHM-9	1.01^{ef}	0.664^{gh}	$3.02^{g\text{-}j}$	2.94^{hi}
SE	0.199	0.070	0.353	0.399
F ratio (df = 12, 80)	4.64	43.3	33.9	37.3

day of salt-stress imposition, respectively, compared to the control condition (Table 2). Similarly, $O_2^{\bullet-}$ contents increased by 46, 239, and 400% in BHM-5; by 17, 87, and 171% in BHM-7; and by 44, 154, and 231% in BHM-9 on the 3rd, 6th, and 9th day of salt-stress, respectively, compared to their respective control conditions (Table 2). On day 9, $O_2^{\bullet-}$ generation was 213, 155, and 159% higher in BHM-5 than in BIL214 × BIL218, BHM-7, and BHM-9, respectively. However, during the recovery period, all genotypes exhibited significant reductions in $O_2^{\bullet-}$ and H_2O_2 contents, with BIL214 × BIL218 showing a remarkable recovery (Table 2).

H_2O_2 contents increased in BIL214 × BIL218 by 46, 129, and 269%; in BHM-5 by 56, 386, and 530%; in BHM-7 by 34, 242, and 351%; and in BHM-9 by 25, 141, and 208% on the 3rd, 6th, and 9th day of salt-stress, respectively, compared to the respective non-stressed control (Table 2). On the 9th day of stress, BHM-5 had 126, 102, and 110% higher H_2O_2 concentration compared to BIL214 × BIL218, BHM-7, and BHM-9, respectively. Similar to $O_2^{\bullet-}$, H_2O_2 contents decreased during the recovery period, with reductions of 64, 68, 61, and 63% in BIL214 × BIL218, BHM-5, BHM-7, and BHM-9 genotypes, respectively, compared to their respective 9th-day salt stress (Table 2).

3.5. Salinity stress altered SOD activities

Salinity stress-induced changes in SOD activities, which were significant in terms of treatments, genotypes, and their interactions (Table 3). The interaction effects revealed that the changes in SOD activity were generally similar in the maize genotypes as the duration of stress progressed. However, on the 9th day, SOD activity remained higher in tolerant genotypes compared to sensitive genotypes in an insignificant manner. Nevertheless, the recovery treatment showed comparable results for SOD activity in all genotypes except for BHM-9 (Table 3).

Three SOD isozymes were detected in this study, with Mn-SOD and Cu/Zn-SOD isozymes being activated in all genotypes, while Fe-SOD was faintly detected. Mn-SOD exhibited its highest activity on the 6th day of salinity treatment, although this activity decreased on day 9. Cu/Zn-SOD activity was consistently higher in the BIL214 × BIL218 genotype. During the recovery period, both Mn- and Cu/Zn-SOD displayed better expressions in BHM-9 (Fig. 2).

Table 3
Effect of salinity stress on CAT, POD, APX, and GPX in maize seedlings at different day intervals of stress treatments. Each value of data represents the mean of five replications ($n = 5$). Values within a column with different letters are significant at $p \leq 0.05$. Details are given in Table 1.

Source of Variation	SOD	CAT	POD	APX	GPX
Treatment					
Control (C)	73.66^{c}	43.78^{c}	0.591^{d}	0.698^{c}	76.74^{a}
Day 3 (3 d)	82.91^{b}	46.75^{b}	0.729^{b}	0.781^{b}	57.65^{c}
Day 6 (6 d)	93.82^{a}	51.34^{a}	0.889^{a}	0.864^{a}	81.20^{a}
Day 9 (9 d)	85.56^{b}	39.26^{d}	0.669^{c}	0.739^{bc}	58.18^{c}
Recovery (R)	83.57^{b}	40.54^{d}	0.690^{bc}	0.778^{b}	63.02^{b}
SE	2.06	1.44	0.025	0.026	2.25
F ratio (df = 4, 80)	24.42	23.01	39.38	11.2	47.2
Genotype					
BIL214 × BIL218	82.84^{b}	44.02^{b}	0.758^{b}	0.802^{a}	60.73^{c}
BHM-5	80.84^{b}	31.29^{c}	0.641^{c}	0.726^{b}	67.33^{b}
BHM-7	82.13^{b}	55.83^{a}	0.805^{a}	0.827^{a}	65.07^{b}
BHM-9	89.81^{a}	46.20^{b}	0.650^{c}	0.733^{b}	76.30^{a}
SE	1.84	1.29	0.022	0.023	2.01
F ratio (df = 3, 80)	9.53	122.9	26.47	9.17	21.3
Interaction					
C × BIL214 × BIL218	71.78^{gh}	30.66^{fg}	0.424^{g}	0.718^{e-h}	77.0^{c-e}
C × BHM-5	74.67^{gh}	42.12^{e}	0.536^{f}	0.672^{gh}	71.34^{ef}
C × BHM-7	70.69^{h}	53.68^{c}	0.787^{c}	0.731^{e-h}	84.66^{a-c}
C × BHM-9	77.50^{f-h}	48.68^{cd}	0.619^{ef}	0.670^{gh}	73.97^{d-f}
3 d × BIL214 × BIL218	83.92^{c-f}	60.61^{b}	0.819^{bc}	0.953^{a}	57.95^{g-i}
3 d × BHM-5	79.34^{e-g}	32.33^{f}	0.583^{ef}	0.702^{f-h}	57.35^{g-i}
3 d × BHM-7	77.68^{f-h}	48.68^{cd}	0.893^{ab}	0.776^{c-f}	41.33^{k}
3 d × BHM-9	90.69^{a-c}	45.39^{de}	0.622^{ef}	0.694^{f-h}	73.99^{d-f}
6 d × BIL214 × BIL218	91.33^{a-c}	49.57^{cd}	0.893^{ab}	0.930^{a}	66.26^{fg}
6 d × BHM-5	93.97^{ab}	25.95^{g}	0.926^{a}	0.816^{b-e}	86.33^{ab}
6 d × BHM-7	91.67^{a-c}	61.56^{b}	0.937^{a}	0.891^{ab}	91.67^{a}
6 d × BHM-9	98.31^{a}	68.29^{a}	0.799^{bc}	0.820^{b-e}	80.54^{b-d}
9 d × BIL214 × BIL218	87.82^{b-d}	46.95^{de}	0.846^{a-c}	0.651^{h}	49.71^{i-k}
9 d × BHM-5	79.90^{d-g}	12.07^{h}	0.613^{ef}	0.677^{f-h}	59.33^{gh}
9 d × BHM-7	86.91^{b-e}	65.67^{ab}	0.656^{de}	0.861^{a-d}	45.33^{jk}
9 d × BHM-9	87.63^{b-d}	32.34^{f}	0.560^{ef}	0.766^{d-g}	78.33^{b-e}
R × BIL214 × BIL218	79.34^{e-g}	32.31^{f}	0.807^{bc}	0.756^{e-g}	52.73^{h-j}
R × BHM-5	76.33^{f-h}	43.98^{de}	0.547^{f}	0.764^{d-g}	62.32^{g}
R × BHM-7	83.69^{c-f}	49.56^{cd}	0.753^{cd}	0.876^{a-c}	62.34^{g}
R × BHM-9	94.92^{ab}	36.33^{f}	0.652^{e}	0.717^{e-h}	74.68^{d-f}
SE	4.12	2.88	0.050	0.052	4.50
F ratio (df = 12, 80)	1.88	38.9	9.32	3.62	10.2

3.6. The activities of H_2O_2-related antioxidant enzymes were regulated by salinity stress

Furthermore, the activities of H_2O_2-related antioxidant enzymes, namely CAT, POD, and APX showed significant variations among treatments, genotypes, and their interactions (Table 3). CAT activity increased in BIL214 × BIL218, BHM-7, and BHM-9 as the stress period progressed, with the highest activity observed in the sensitive genotype BHM-5. However, on day 7 of salt treatment, BHM-7 maintained higher CAT activity than BIL214 × BIL218 and BHM-9. Conversely, CAT activity decreased significantly in BHM-5, and on day 9, BHM-7, BIL214 × BIL218, and BHM-9 showed 444, 289, and 168% higher CAT activity than BHM-5 (Table 3). The in-gel native activity analysis supported these results, revealing the presence of three CAT isozymes, with CAT3 being denser than CAT2 and CAT1 in all the genotypes (Fig. 4).

POD activity increased by 93, 111, and 100% in the BIL214 × BIL218 genotype on days 3, 6, and 9 of stress treatment, respectively, compared to its control. In contrast, BHM-5 showed increases of 9, 73, and 14% in POD activity during the same period. Interestingly, on days 3 and 6 of salt treatment, genotypes BHM-7 and BHM-9 displayed increasing tendencies in POD activity (in BHM-7 by 14 and 19%, and in BHM-9 by 1 and 29%, respectively), but this activity decreased on day 9 by 17 and 10%, respectively, compared to their respective control conditions (Table 3). On day 9, BIL214 × BIL218 exhibited better POD activity than other genotypes. During the recovery stage, BIL214 × BIL218, BHM-7, and BHM-9 showed higher activity than BHM-5 (Table 3). Among the three POD isozymes, POD3 was highly activated in the BHM-5 genotype, while POD2 and POD1 were activated in the BHM-9 and BIL214 × BIL218 genotypes, respectively (Fig. 2D).

APX activity was notably higher in the BIL214 × BIL218 genotype up to day 6 of stress, with APX1 and APX2 isozymes being conspicuous in this genotype (Table 3 and Fig. 2C). After 6 days of stress, APX activity decreased in BIL214 × BIL218 to levels statistically similar to BHM-5, while it increased in BHM-7 and BHM-9 compared to BHM-5. On day 6 of salt treatment, APX activity increased by 30, 21, 22, and 22% in BIL214 × BIL218, BHM-5, BHM-7, and BHM-9 genotypes, respectively, compared to their respective control conditions. However, on day 9, APX activity decreased by 9% in BIL214 × BIL218 and increased by 1, 18, and 14% in BHM-5, BHM-7, and BHM-9 genotypes, respectively. During the recovery period, APX activity increased by 16, 13, and 2% in BIL214 × BIL218, BHM-5, and BHM-7 genotypes, respectively, while it decreased by 6% in BHM-9 compared to the final day of salt stress treatment for each genotype (Table 3). Native in-gel activity analysis showed four APX isozymes, with APX1 and APX2 appearing in BIL214 × BIL218, which may be important in stress and recovery.

The activity of glutathione peroxidase (GPX) exhibited significant variations among genotypes, treatments, and their interactions

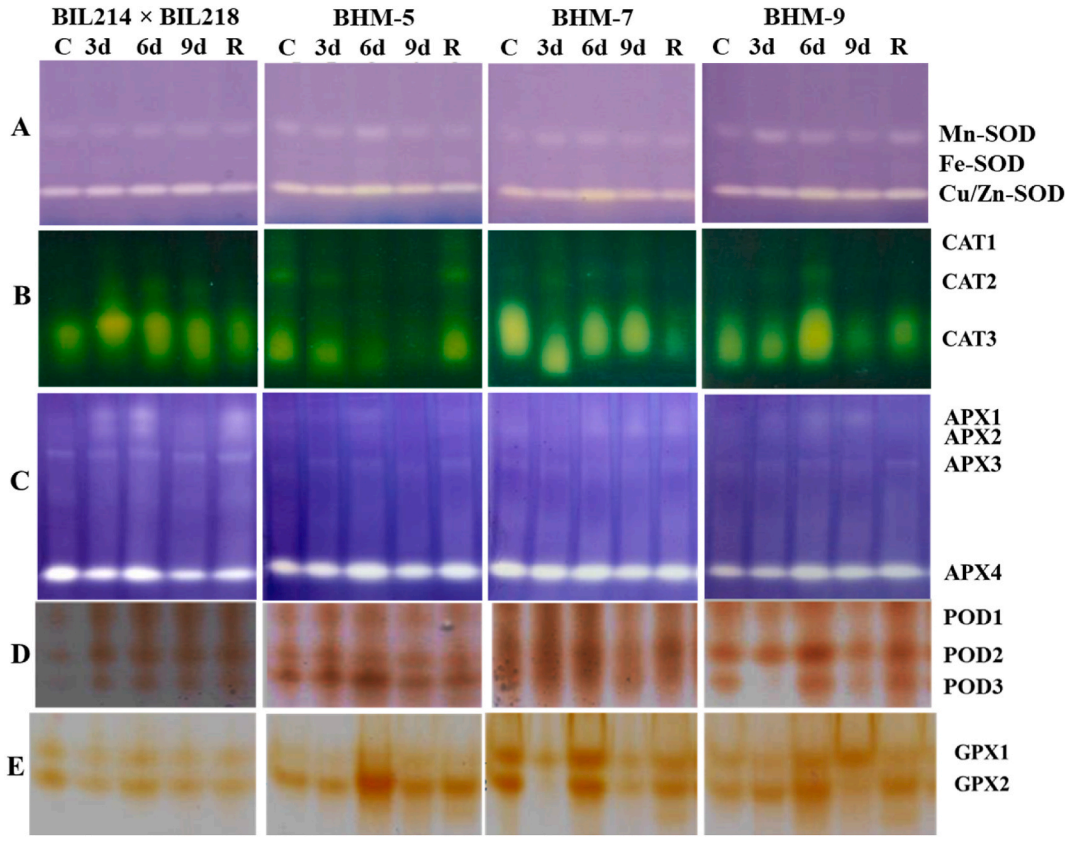

Fig. 2. Native in-gel activity of ROS metabolizing enzymes in maize. For SOD, 10% and for CAT, APX, POD and GPX, 8% SDS-PAGE were used. In each lane 50 μg protein was used.

(Table 3). The interaction effects revealed that the activity changed differently in various genotypes as the stress duration progressed. Interestingly, as the stress duration increased, GPX activity became higher in BHM-9, setting it apart from the other genotypes. What's particularly intriguing is that the trend in GPX activity differs from that of the control condition. In most genotypes, GPX activity decreased under salt stress conditions compared to the control, except for the BHM-9 genotype, which showed a consistent and comparable level of GPX activity throughout the treatment period (Table 3). This trend in GPX activity was supported by in-gel activity analysis, which identified two isozymes of GPX activity (Fig. 2E). Isozyme 2 (GPX2) was notably more activated in comparison to GPX1, suggesting its potential importance in the response to salt stress and the observed differences among genotypes.

3.7. Glutathione-related metabolism regulation under salinity stress in maize

We measured the activity of GR in different genotypes under salt stress and compared it to the control conditions. We found that GR activity increased in all genotypes, but at different rates and times (Table 4). The BIL214 × BIL218 genotype had the highest GR activity, which increased by 53% and 115% on the 6th and 9th days of salt stress, respectively. The BHM-5 genotype had the lowest GR activity, which increased by 4, 12, and 34% on the 3rd, 6th, and 9th days of salt stress, respectively. The BHM-7 and BHM-9 genotypes had similar GR activity, with the mean increases of 4., 39, and 83% on the same days of salt stress, respectively (Table 4, Figure A4). Notably, on day 9, BIL214 × BIL218 displayed significantly higher GR activity compared to the sensitive genotype (Table 4). This suggests a robust stress response mechanism involving GR in this tolerant genotype.

During the recovery treatment, all the genotypes showed a notable recovery from stress, as indicated by lower GR activity. For instance, compared to the 9th day of stress treatment, GR activity decreased by 37% in BIL214 × BIL218, 31% in BHM-5, 31% in BHM-7, and 20% in BHM-9 (Table 4).

Moreover, salinity stress led to a decrease in the levels of reduced glutathione (GSH) and its redox state in all the genotypes. Higher oxidation of GSH was observed in BHM-5, leading to higher levels of oxidized glutathione (GSSG) (Table 4). After three days of stress

Table 4
Effect of salinity stress on GR, GSH, MDHAR, DHAR, and ASA in maize seedlings at different day intervals of stress treatments. Each value of data represents the mean of five replications ($n = 5$). Values within a column with different letters are significant at $p \leq 0.05$. Details are given in Table 1.

Source of Variation	GR	GSH	MDHAR	DHAR	ASA
	(μmol min^{-1} mg^{-1} Protein)	(redox homeostasis)	(nmol min^{-1} mg^{-1} Protein)		(redox homeostasis)
Treatment					
Control (C)	45.99^{d}	0.760^{a}	54.29^{d}	42.43^{d}	0.776^{a}
Day 3 (3 d)	46.91^{d}	0.693^{b}	63.10^{c}	57.84^{c}	0.663^{b}
Day 6 (6 d)	62.22^{b}	0.598^{c}	81.78^{a}	72.75^{a}	0.584^{c}
Day 9 (9 d)	81.65^{a}	0.469^{d}	71.07^{b}	67.72^{b}	0.517^{d}
Recovery (R)	56.90^{c}	0.582^{c}	65.15^{c}	61.12^{c}	0.598^{c}
SE	1.91	0.025	2.43	1.85	0.021
F ratio (df = 4, 80)	114.9	40.8	35.1	78.3	44.6
Genotype					
BIL214 × BIL218	62.86^{a}	0.643^{a}	71.23^{ab}	62.03^{a}	0.672^{a}
BHM-5	54.15^{c}	0.577^{b}	55.01^{c}	56.78^{b}	0.571^{c}
BHM-7	58.59^{b}	0.628^{a}	68.66^{b}	60.50^{a}	0.635^{ab}
BHM-9	59.35^{b}	0.634^{a}	73.41^{a}	62.17^{a}	0.633^{b}
SE	1.712	0.022	2.18	1.66	0.019
F ratio (df = 3, 80)	8.75	3.55	28.9	4.61	10.1
Interaction					
C × BIL214 × BIL218	45.05^{jk}	0.769^{a}	51.11^{ij}	46.80^{ij}	0.827^{a}
C × BHM-5	49.9^{i-k}	0.728^{ab}	46.77^{j}	41.30^{j}	0.762^{ab}
C × BHM-7	46.00^{jk}	0.764^{a}	56.68^{hi}	39.80^{j}	0.750^{ab}
C × BHM-9	43.04^{k}	0.780^{a}	62.61^{f-h}	41.80^{j}	0.764^{ab}
3 d × BIL214 × BIL218	42.92^{k}	0.720^{ab}	62.83^{e-h}	60.80^{e-g}	0.667^{cd}
3 d × BHM-5	51.99^{h-j}	0.650^{b-e}	53.89^{h-j}	54.90^{f-h}	0.616^{d-f}
3 d × BHM-7	47.96^{jk}	0.696^{a-d}	62.49^{f-h}	54.50^{gh}	0.704^{bc}
3 d × BHM-9	44.80^{jk}	0.708^{a-c}	73.20^{b-d}	61.18^{e-g}	0.664^{c-e}
6 d × BIL214 × BIL218	69.00^{c}	0.610^{d-f}	87.33^{a}	75.30^{ab}	0.616^{d-f}
6 d × BHM-5	55.91^{g-i}	0.560^{e-h}	71.33^{c-f}	79.30^{a}	0.511^{h}
6 d × BHM-7	59.01^{e-h}	0.609^{d-f}	82.20^{ab}	62.20^{d-f}	0.609^{d-f}
6 d × BHM-9	64.96^{c-e}	0.613^{c-f}	86.26^{a}	74.21^{ab}	0.602^{d-g}
9 d × BIL214 × BIL218	96.67^{a}	0.499^{g-i}	82.43^{ab}	81.49^{a}	0.582^{e-h}
9 d × BHM-5	70.00^{cd}	0.420^{i}	45.35^{j}	49.49^{hi}	0.421^{i}
9 d × BHM-7	82.96^{b}	0.480^{hi}	78.62^{a-c}	75.70^{ab}	0.523^{gh}
9 d × BHM-9	79.95^{b}	0.476^{hi}	77.90^{a-c}	64.18^{c-e}	0.542^{f-h}
R × BIL214 × BIL218	60.67^{d-g}	0.617^{c-f}	72.46^{c-e}	45.79^{ij}	0.666^{cd}
R × BHM-5	45.93^{jk}	0.529^{f-h}	57.71^{g-i}	58.91^{e-g}	0.546^{f-h}
R × BHM-7	57.00^{f-i}	0.590^{e-g}	63.33^{e-h}	70.31^{bc}	0.588^{d-h}
R × BHM-9	63.98^{c-f}	0.594^{e-g}	67.10^{d-g}	69.49^{b-d}	0.593^{d-g}
SE	3.83	0.049	4.86	3.70	0.041
F ratio (df = 12, 80)	6.95	1.87	3.32	13.7	2.14

treatment, GSH redox homeostasis decreased by 6, 11, 9, and 9% in BIL214 × BIL218, BHM-5, BHM-7, and BHM-9 genotypes, respectively, compared to their controls. On day 6, it further decreased by 21, 23, 20, and 21%. By the final day, decreases reached 35, 42, 37, and 39%, respectively. Importantly, during the recovery phase, GSH redox homeostasis significantly increased in all genotypes, ranging from 23 to 26%, compared to the 9th day of salt stress treatment (Table 4).

3.8. Ascorbate-related metabolism regulation under salinity stress in maize

Salinity stress led to a significant increase in the activities of MDHAR and DHAR in all genotypes, except for BHM-5, which had a drastic decrease at day 9. The BIL214 × BIL218 genotype had the highest activity of these enzymes, while the BHM-5 genotype had the lowest. During the recovery treatment, MDHAR and DHAR activities increased in BHM-5, but DHAR activity decreased by 43.8% in BIL214 × BIL218 compared to day 9 of salt stress (Table 4).

Salinity stress decreased ascorbate (ASA) content and its redox state in all genotypes (Table 4). BHM-5 exhibited higher ASA oxidation, leading to increased dehydroascorbate (DHA) with stress duration. Compared to the control, ASA redox homeostasis decreased by 19, 33, and 45% at 3, 6, and 9 days, respectively in BHM-5. BIL214 × BIL218 showed smaller declines of 10, 20, and 30% at the same time points. Similarly, BHM-7 and BHM-9 displayed mean decreases of 19, 25, and 33% at 3, 6, and 9 days, respectively. Importantly, withdrawing salt stress accelerated ASA redox homeostasis recovery, with increases ranging from 9 to 30% compared to day 9 values (Table 4).

Additionally, GST activity and proline content (Pro) were measured in the leaves (Table S1). Significant differences were observed for treatment, genotype, and their interaction. Both parameters increased with stress duration. Although GST activity was found to be higher in the sensitive genotype BHM-5, the tolerant genotypes, especially BIL214 × BIL218, maintained higher proline content, which increased with stress duration throughout the study period.

Table 5
Effect of salinity stress on MG, Gly I, and Gly II in maize seedlings at different day intervals of stress treatments. Each value of data represents the mean of five replications ($n = 5$). Values within a column with different letters are significant at $p \leq 0.05$. Details are given in Table 1.

Source of Variation	MG	Gly I	Gly II
	(μmol g^{-1} FW)	(μmol min^{-1} mg^{-1} protein)	
Treatment			
Control (C)	7.90^{d}	0.477^{c}	0.101^{d}
Day 3 (3 d)	16.41^{c}	0.754^{b}	0.159^{b}
Day 6 (6 d)	28.82^{b}	0.922^{a}	0.177^{a}
Day 9 (9 d)	33.02^{a}	0.963^{a}	0.167^{ab}
Recovery (R)	15.48^{c}	0.477^{c}	0.135^{c}
SE	0.782	0.028	7.76
F ratio (df = 4, 80)	348.7	137.8	30.5
Genotype			
BIL214 × BIL218	16.24^{d}	0.737^{b}	0.169^{a}
BHM-5	24.84^{a}	0.599^{c}	0.138^{b}
BHM-7	18.76^{c}	0.734^{b}	0.141^{b}
BHM-9	21.46^{b}	0.804^{a}	0.143^{b}
SE	0.70	0.025	6.94
F ratio (df = 3, 80)	55.6	23.2	8.70
Interaction			
C × BIL214 × BIL218	7.10^{i}	0.449^{i}	0.110^{fg}
C × BHM-5	9.80^{i}	0.410^{i}	0.089^{g}
C × BHM-7	6.80^{i}	0.470^{hi}	0.103^{g}
C × BHM-9	7.89^{i}	0.580^{gh}	0.103^{g}
3 d × BIL214 × BIL218	13.52^{h}	0.758^{ef}	0.168^{bc}
3 d × BHM-5	17.73^{e-g}	0.680^{e-g}	0.180^{b}
3 d × BHM-7	15.67^{f-h}	0.787^{de}	0.150^{b-e}
3 d × BHM-9	18.70^{ef}	0.791^{de}	0.140^{c-f}
6 d × BIL214 × BIL218	19.88^{e}	0.980^{bc}	0.220^{a}
6 d × BHM-5	36.69^{b}	0.790^{de}	0.160^{b-d}
6 d × BHM-7	26.49^{d}	0.890^{cd}	0.159^{b-d}
6 d × BHM-9	32.20^{c}	1.027^{ab}	0.170^{bc}
9 d × BIL214 × BIL218	23.81^{d}	1.020^{ab}	0.230^{a}
9 d × BHM-5	43.30^{a}	0.666^{fg}	0.120^{e-g}
9 d × BHM-7	31.29^{c}	1.036^{ab}	0.158^{b-d}
9 d × BHM-9	33.70^{bc}	1.130^{a}	0.160^{b-d}
R × BIL214 × BIL218	16.88^{e-g}	0.480^{hi}	0.120^{e-g}
R × BHM-5	16.67^{fg}	0.449^{i}	0.140^{c-f}
R × BHM-7	13.53^{h}	0.489^{hi}	0.136^{d-f}
R × BHM-9	14.82^{gh}	0.490^{hi}	0.143^{c-e}
SE	1.56	0.056	0.016
F ratio (df = 12, 80)	12.1	3.77	4.92

3.9. Regulation of methylglyoxal by activities of Gly I and Gly II under salinity stress

The MG concentration and glyoxalase activities in leaves of different genotypes under salt stress were compared to the control conditions (Table 5). Salt stress increased the cytotoxic MG levels in all genotypes, but at different rates and times. The BIL214 × BIL218 genotype showed the lowest MG levels, which increased by 90, 180, and 235% on the 3rd, 6th, and 9th days of salt stress, respectively. The BHM-5 genotype had a pronounced surge in MG levels, which increased by 81, 274, and 342% on the same days of salt stress, respectively. The BHM-7 and BHM-9 genotypes had the similar trend in the increases of MG levels, averaging 133, 299, and 343% on the same days of salt stress, respectively. Notably, BHM-5 had the highest MG content on day 9, which was 82% higher than BIL214 × BIL218, 52% higher than BHM-7, and 29% higher than BHM-9. MG content decreased in all genotypes during the recovery phase. The BHM-7 genotype had the highest decrease of 62%, followed by BHM-9 with 56%, BHM-5 with 57%, and BIL214 × BIL218 with 29% compared to their respective day 9 levels (Table 5).

Both glyoxalase I (Gly I) and II (Gly II) activities significantly increased under salt stress (Table 5). BIL214 × BIL218 exhibited the most pronounced rise in both enzymes compared to other genotypes. Interestingly, BHM-5 displayed consistently lower activities throughout the study period. Specifically, on the 3rd day of salt stress, Gly I activity surged by 69% in BIL214 × BIL218, followed by BHM-9 (68%), BHM-7 (66%), BHM-5 (36%), and. This trend continued on the 6th and 9th days, with BIL214 × BIL218 maintaining the highest increases (118 and 127%, respectively). During the recovery phase, however, Gly I activity declined in all genotypes, compared to 9th days of stress treatment (Table 5).

Gly II activity also responded significantly to salt stress, with BIL214 × BIL218 again showing the highest increases (52, 100, and 109% on days 3, 6, and 9, respectively) compared to other genotypes. BHM-5 initially displayed a strong response but exhibited a lower increase on day 9 (34%). The other genotypes showed moderate increases throughout the stress period. Interestingly, while BIL214 × BIL218 and BHM-9 experienced a decrease in Gly II activity during recovery, BHM-5 showed a slight increase (17%). BHM-7 maintained relatively stable activity levels throughout the recovery phase (Table 5).

3.10. Correlation between NADPH oxidase and other traits

NADPH oxidase (NOX) activity was differentially associated with ROS, antioxidants, and redox homeostasis in the tolerant, moderate-tolerant, and sensitive genotypes (Fig. 3). In the tolerant genotype BIL214 × BIL218, NOX activity was significantly correlated with all other traits, followed by the moderate-tolerant genotypes BHM-7 and BHM-9, which showed a non-significant relationship with POD activity, while in the sensitive genotype BHM-5, NOX activity was not significantly correlated with POD, APX, and GPX activity (Fig. 3). Interestingly, NOX activity was more strongly and positively associated with Na^+/K^+, $O_2^{\bullet-}$, H_2O_2, and negatively with redox homeostasis in the sensitive genotype BHM-5 than that of the tolerant genotypes (Fig. 3), implying that higher ROS generation and disrupted redox homeostasis of the genotype were governed by higher NOX activity. Conversely, the tolerant genotype BIL214 × BIL218 exhibited stronger positive associations with NOX activity and antioxidant enzymes, except GPX, and weaker negative relations with redox homeostasis in comparison with the sensitive BHM-5 (Fig. 3), indicating that the tolerant genotype possesses a better ability to effectively detoxify the accumulated NOX and ROS to maintain the redox homeostasis. Nevertheless, a stronger and negative association between NOX and CAT was observed in the sensitive genotype, while this association was positive for the tolerant and moderate-tolerant genotypes (Fig. 3).

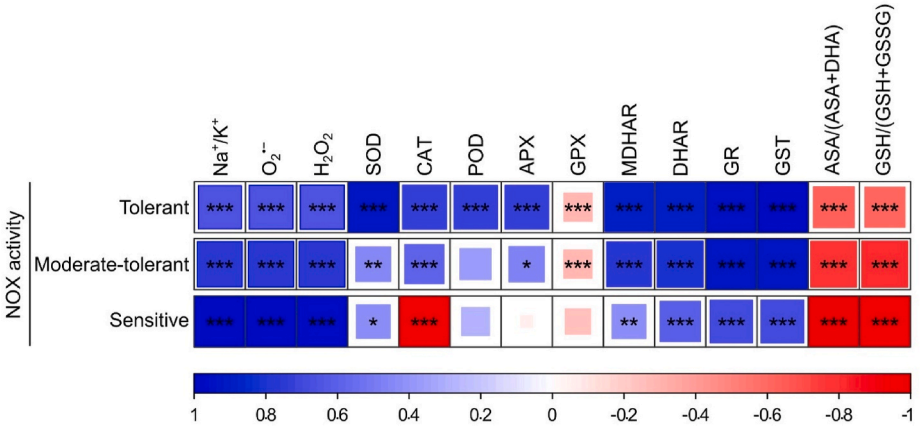

Fig. 3. Correlations between NADPH oxidase (NOX) activity and other traits of the tolerant, moderate-tolerant, and sensitive maize genotypes imposed to salt stress. The correlation coefficient increases as the size and color intensity of the squares increase. *, **, and *** indicate the association is significant at $p < 0.05$, <0.01, and <0.001, respectively. Details are given in Table 1. (For interpretation of the references to color in this figure legend, the reader is referred to the Web version of this article.)

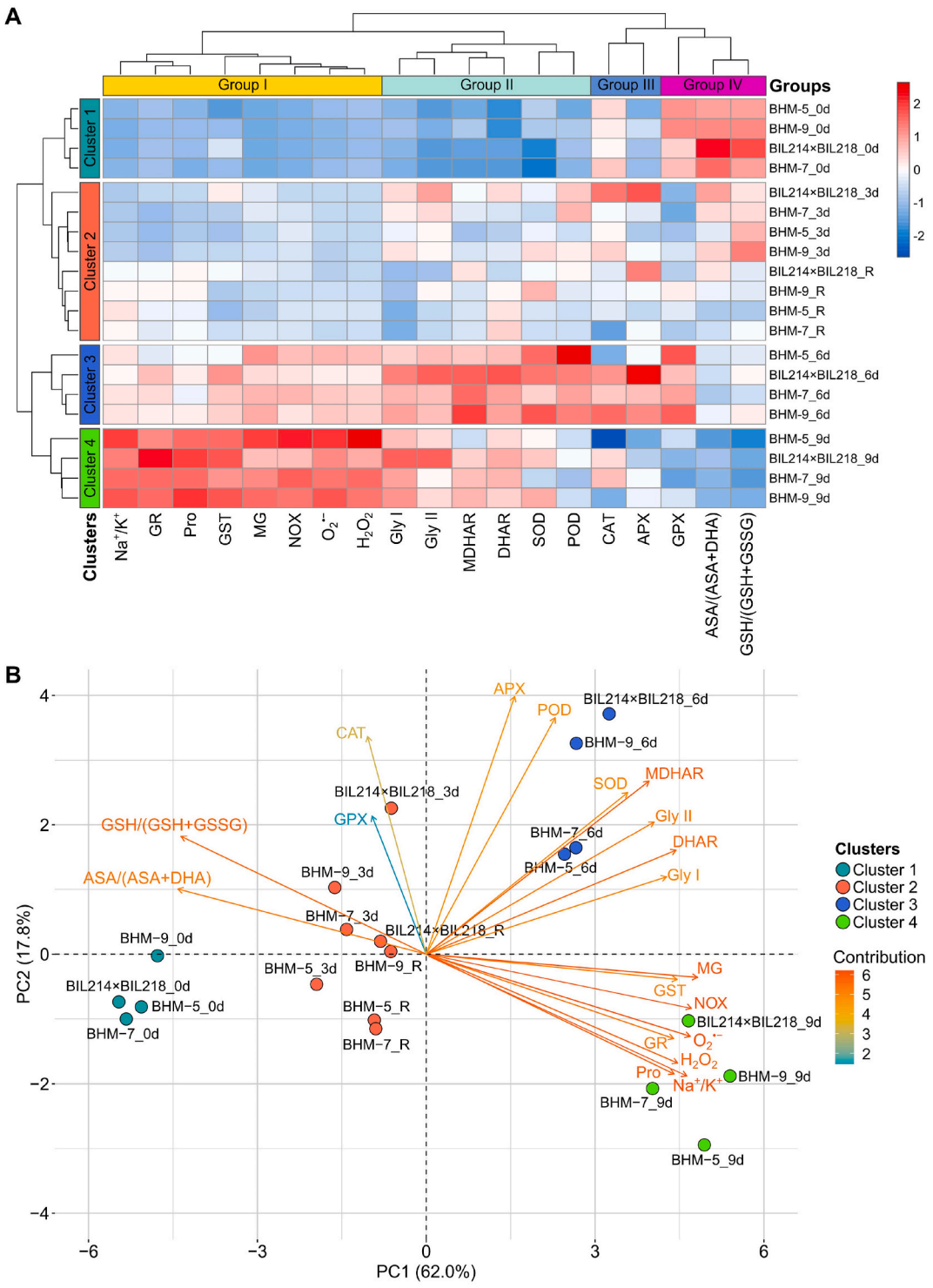

Fig. 4. Heatmap-cluster (A) and principal component analysis [PCA]-biplot (B) of the maize genotypes-days after salt stress induction *vs* studied traits. Details are given in Table 1.

3.11. Relation assessment of responses across treatments vs. traits

A comparative analysis of the heatmap revealed four distinct groups among the parameters studied (Fig. 4). Group I included oxidative stress indicators (MG, NOX, ROS), Na^+/K^+ levels, GR, GST, and proline, while Group IV consisted of GSH and ASA redox homeostasis, as well as GPX. Group II and Group III contained most of the ROS and MG metabolizing enzymes, including MDHAR and DHAR. Groups I and IV clearly showed an opposite relationship, where NOX, ROS, and MG increased with Na^+ accumulation, while GSH and ASA redox homeostasis decreased with the duration of stress (Fig. 4). Additionally, the heatmap indicated that most of the ROS and MG metabolizing enzyme activities, falling within Groups II and III, were higher on day 6 (Cluster 3) of stress. The color contrast within Cluster 4 indicated that compared to other genotypes on day 9, BHM-5 exhibited the maximum Na^+, NOX, ROS, and MG concentrations, along with the least glyoxalases and ROS scavenging machinery (Fig. 4).

3.12. Principal component analysis (PCA)

Principal Component Analysis (PCA) of the maize seedlings' responses to salt stress duration revealed a total of four principal components (PCs), but the first two PCs exhibited eigenvalues >1 and were significant. The first two PCs explained approximately 80% of the variability in salt stress (Fig. 4 and Table S2). The PCA biplot showed that PC1 accounted for 62% of the total variability and contributed positively via Na^+/K^+, NOX, ROS, GR, GST, MDHAR, DHAR, MG, Pro, glyoxalases, and SOD, while it contributed negatively via ASA- and GSH homeostasis, CAT, and GPX (Fig. 4 and Table S2). The second PC accounted for about 18% of the total variation and was mainly contributed to by APX, POD, CAT, MDHAR, and SOD, as well as GPX, glyoxalases, DHAR, and the homeostasis of ASA and GSH.

4. Discussion

4.1. Screening of relatively salt-tolerant and sensitive genotypes

Salinity poses a significant threat to global food security and natural biodiversity. Plants rely on ROS-mediated signaling networks to adapt to salt stress, which regulates various physiological and molecular processes [3]. Growth inhibition and biomass reduction are common consequences of salinity-induced stress in plants [77]. In the present study, the detrimental effects of soil salinity on growth were evident as reductions in growth for all genotypes (Fig. 1). Notably, BHM-5 genotype exhibited the most pronounced growth reduction, while the BIL214 × BIL218 genotype displayed remarkable salt stress tolerance (Fig. 1). To evaluate salt tolerance, the accumulation of reactive oxygen species (ROS) and their metabolic product malondialdehyde (MDA) were used as important biochemical markers [78,79]. Our results indicated that the accumulation of superoxide ($O_2^{\bullet-}$) and hydrogen peroxide (H_2O_2) and MDA content significantly increased in the leaves of all maize genotypes after 30 days of salt treatment, with the highest levels observed in BHM-5 (Figs. S1A, B, C). This strongly supported the notion that growth reduction was associated with increased oxidative stress in BHM-5 compared to the other genotypes. Therefore, an effective screening approach was validated using phenotyping and biochemical markers indicative of stress. Additionally, the production of ROS is closely linked to the activity of NADPH oxidase (NOX), a plasma membrane-bound enzyme encoded by *RBOH* genes [4]. Our study revealed a positive correlation between NOX activity and ROS production, as observed through spectrophotometry and native in-gel electrophoretic activity (Figs. S1D and E), with two prominent isozymes intensifying in salt-sensitive maize genotypes. Consequently, we conducted further investigations to explore the interrelationships among ionic balance (Na^+/K^+), NOX induction, ROS generation, antioxidants, and the glyoxalase system in the selected genotypes.

4.2. Na^+ accumulation, NOX induction, ROS generation, antioxidants, and glyoxalase system

ROS can be generated through both enzymatic and non-enzymatic pathways, with NADPH oxidases being the most widely recognized enzymes responsible for ROS production [80]. NADPH oxidase, a complex enzyme, transports electrons across membranes, usually the plasma membrane, from a cytosolic electron donor to oxygen in the extracellular space, resulting in the generation of $O_2^{\bullet-}$ [81]. Various members of the respiratory burst oxidase homolog (RBOH) family have been identified in plants, including *Arabidopsis*, rice, tomato, potato, tobacco, and maize [82–87]. Several studies have highlighted the crucial role of plasma membrane NADPH oxidase in the physiological and molecular adaptation of plants to salinity, particularly in regulating Na^+/K^+ homeostasis and the induction of antioxidative enzymes in response to NaCl [37,88]. In our second study, maize genotypes exposed to salinity exhibited substantial increases in Na^+/K^+ levels, $O_2^{\bullet-}$ and H_2O_2 generation, and a concomitant rise in MDA content in the leaves (Table 2). These results are in line with previous studies that reported a positive correlation between NADPH oxidase activity [80] and $O_2^{\bullet-}$ levels [49], and increased NADPH oxidase activity with H_2O_2 production in cucumber roots under salinity [55]. The toxic effects resulting from excessive $O_2^{\bullet-}$ production can be mitigated by SOD activity, which rapidly converts $O_2^{\bullet-}$ to H_2O_2 [89]. Cultivar differences in cucumber have also been reported regarding the accumulation of NADPH oxidase activity along with H_2O_2 [90]. In our previous study, we observed that salt-sensitive maize seedlings exhibited higher ROS production [57]. In this study, the sensitive maize genotype BMH-5 displayed higher Na^+/K^+ levels along with increased NADPH oxidase, $O_2^{\bullet-}$, and H_2O_2 in fully expanded maize leaves. Additionally, Rodríguez et al. [52] reported salt-induced decreases in NADPH oxidase activity in the elongation zone of maize leaves when NaCl was gradually increased (25 mM-50 mM-100 mM–150 mM) until it reached 150 mM. This difference may be attributed to genotype-specific factors or robust tissue-specific responses [49]. The data revealed that subsequent decreases in $O_2^{\bullet-}$ and H_2O_2 contents were associated

with reduced NADPH oxidase activity when the seedlings were grown in a saline-free Hoagland medium (Table 2). Similar observations were made during the recovery stage, with lower NADPH oxidase activity coinciding with decreased Na^+/K^+ levels (Table 2), suggesting a positive relationship between Na^+/K^+ and NADPH oxidase.

During salt stress, we observed a parallel relationship between NADPH oxidase and superoxide production (Fig. S1 and Table 2). Superoxide dismutase (SOD) serves as the primary protector by scavenging $O_2^{\bullet-}$, and its activity is crucial for mitigating the toxic effects of $O_2^{\bullet-}$ [91]. Interestingly, increased SOD activity correlated with elevated NOX activity. As we know, NOX produces extracellular $O_2^{\bullet-}$ upon activation under salt stress, both at the transcriptional and functional levels [33,37]. The generated $O_2^{\bullet-}$ is then rapidly converted into less harmful substances by SOD [39].

This relationship explains the increased SOD and NOX activities observed in our study. However, the overaccumulation of $O_2^{\bullet-}$ and H_2O_2 in BHM-5 suggests overexpression of SOD and NOX in this genotype. The enzyme SOD exists as three isozymes in plant cells: Mn-SOD in mitochondria and peroxisomes, Cu/Zn-SOD in the cytosol, mitochondria, and plastids, and Fe-SOD in the cytosol, mitochondria, chloroplasts, and peroxisomes [92]. Although Fe-SOD was not prominent in our study (Fig. 2A), isozymes of Mn-SOD and Cu/Zn-SOD were detected in all maize genotypes, with Cu/Zn-SOD continuously increasing in the tolerant genotype BIL214 × BIL218, indicating better protection against $O_2^{\bullet-}$-mediated oxidative damage during salt stress. This observation aligns with the notion that increased SOD activity is associated with salt tolerance [93].

A lower concentration of H_2O_2 functions as a signaling molecule in signal transduction pathways in response to environmental stresses and plays a role in growth and development processes. However, excessive accumulation of H_2O_2 can lead to oxidative stress in the cell [94]. The relationship between NADPH oxidase and H_2O_2 has been documented in studies involving cucumber [55] and rice [53]. In our study, we also observed higher H_2O_2 levels in conjunction with Na^+/K^+ and NAPDH oxidase activities (Fig. S1 and Table 2) and found a strong correlation between the molecules, with the strongest in sensitive genotype (Fig. 3). It's worth noting that H_2O_2 levels may not always be correlated with NADPH oxidase and superoxide dismutase (SOD) because H_2O_2 can also be produced through non-enzymatic pathways [94].

Excess H_2O_2 can disrupt the functions of enzymes containing thiol groups at their active sites or regulatory domains. Many proteins related to photosynthesis rely on redox regulation mediated by thiols, making it crucial to reduce the accumulation of excess H_2O_2 in cells under adverse conditions to prevent interference with the redox regulation of enzyme activity [95]. To combat the harmful effects of H_2O_2, plants employ various antioxidant enzymes, including catalase (CAT), peroxidase (POD), ascorbate peroxidase (APX), and glutathione peroxidase (GPX).

Among the studied antioxidant enzymes, CAT is located in peroxisomes and specializes in scavenging photorespiratory H_2O_2 [96]. CAT is a potent antioxidant enzyme with a high turnover rate and a low affinity for H_2O_2. This might be due to its independence of substrate [93]. However, in our study, we detected three CAT isozymes in all maize genotypes, with CAT3 being the most prominent (Fig. 2B). Notably, the lowest CAT activity after three days of salt stress in the sensitive genotype BHM-5 likely contributed to the dysregulation of H_2O_2 metabolism, leading to significantly higher H_2O_2 levels in this genotype under salt stress. Previous studies have reported higher CAT activity in salt-tolerant plants compared to sensitive ones in various plant species [93].

APX, on the other hand, is primarily responsible for regulating H_2O_2 levels in the cytosol and chloroplasts. It exhibits a high affinity for H_2O_2 compared to CAT and other enzymes, and it is frequently employed by plants to fine-tune H_2O_2 levels [97]. In our study, the native in-gel activity of APX increased in all genotypes under salt stress compared to the control, with the highest activity detected on the 6th day of salt stress imposition, which then decreased on the 9th day (Fig. 2C). This suggests that APX plays a role in breaking down H_2O_2 regardless of salt sensitivity. Moreover, during the recovery stage, APX activity increased in all maize genotypes. Similar increases in APX activity under salt stress have been reported in wheat plants [50], *Cucumis sativus*, and *Brassica juncea* [98,99]. Interestingly, APX1 and APX2 were prominently expressed on the 6th day of salinity stress and during recovery in the tolerant genotype BIL214 × BIL218 (Fig. 2C), suggesting their potential importance in salt tolerance.

In a study by Zeeshan et al. [100], a comparison of wheat and barley cultivars concluded that higher activities of antioxidants, including CAT, APX, and POD, are strongly correlated with greater salt tolerance, emphasizing the crucial role of antioxidant activities in mitigating salt-induced oxidative stress. Similarly, Alzahrani et al. [101] found increased levels of SOD and CAT in faba bean genotypes when H_2O_2 levels increased by more than 90% compared to the control under salt stress, confirming the regulation of the antioxidant response under salt stress and its role in mitigating oxidative stress.

Besides CAT and APX, POD and GPX also contribute to H_2O_2 detoxification. PODs are present in various plant cell compartments and the apoplast, where they scavenge H_2O_2 [102]. Many isoenzymes of GPX exist in plant tissues, localized in vacuoles, the cell wall, and the cytosol [103]. Our study detected three POD isozymes (Fig. 2D). Their activity increased gradually with stress duration and recovery, especially in the tolerant genotype BIL214 × BIL218, indicating the importance of POD in H_2O_2 detoxification during salt stress. Conversely, POD activity decreased, particularly after the 6th day of stress, in BHM-5 and BHM-7, while BHM-9 exhibited higher activity than the control on the 6th day of stress and during recovery (Fig. 2D). Two GPX isozymes were found in maize leaves (Fig. 2E), with native gel activity revealing a sharp decrease in GPX activity in the sensitive genotype BHM-5 during prolonged salt stress. This decline in GPX activity likely compromised H_2O_2 metabolism over the long term. Similar to maize, salinity stress has been shown to increase POD activity in cucumber [104], wheat, and barley [100] as well as POD and GPX activity in mung bean [63]. Attia et al. [105] also reported higher activities of POD and GPX in relatively tolerant tomato genotypes.

Glutathione (GSH) is a non-enzymatic antioxidant, and glutathione reductase (GR) regenerates oxidized glutathione (GSSG) to GSH through the Asada–Halliwell–Foyer cycle [106]. Additionally, glutathione S-transferases (GSTs) conjugate GSH to various substrates, including toxic xenobiotics and oxidatively produced compounds [107]. Given the important roles of GSH as redox buffers in cells, we investigated GR activity under salt stress conditions. The highest GR activity was observed on the 9th day of salt treatment, indicating increased utilization of GSH for redox regulation. In wheat, GR activity increased 2.16-fold under salt stress, concomitant with a

1.46-fold increase in GSH levels compared to the control [50]. In our study, the BIL214 × BIL218 genotype displayed a higher GSH redox state, supported by its increased GR activity, suggesting better salt tolerance (Table 3). This is consistent with the role of ASA and GSH in the ascorbate-glutathione cycle, which is vital for plant stress tolerance [89,108]. Furthermore, GSH plays a protective role in salt tolerance by maintaining the redox state [109]. The increased GSH pool is generally considered a protective response against oxidative stress. GR is essential for maintaining a high GSH ratio in plant cells and accelerating H_2O_2 scavenging [89]. While the activity of GR increased under salt stress in our study, it was notably higher in the BIL214 × BIL218 genotype, indicating better maintenance of GSH and GSH-redox levels, whereas BHM-5 exhibited lower GR activity and a lower GSH redox state compared to other genotypes, signifying its sensitiveness to salt stress (Table 3).

Ascorbate (ASA) is the most abundant low-molecular-weight antioxidant that plays a key role in defending against oxidative stress resulting from elevated ROS levels. ASA is also crucial for the removal of H_2O_2 via the ASA-GSH cycle [110]. The oxidation of ASA occurs in two sequential steps, first producing monodehydroascorbate (MDHA) and subsequently dehydroascorbate (DHA). In the ASA-GSH cycle, two molecules of ASA are used by APX to reduce H_2O_2 to water, generating MDHA in the process. MDHA is a radical with a short lifetime and can spontaneously dismutated into DHA and ASA or be reduced to ASA by the NADP(H)−dependent enzyme monodehydroascorbate reductase (MDHAR) [111]. In our study, we observed increased oxidation of ASA in BHM-5 was higher, while the BIL214 × BIL218 genotype effectively maintained a high ASA redox state (Table 3). MDHAR activity, however, remained relatively consistent across all genotypes, with no significant variation (Table 3). This result aligns with our findings regarding NOX activity, as MDHAR is an NADP(H)-dependent enzyme and NOX activity was significantly higher, potentially suppressing MDHAR activity (Table 3). Conversely, dehydroascorbate reductase (DHAR) activity was significantly higher in BHM-5 on the 9th day of salt stress compared to other genotypes (Table 3). Upregulation of DHAR activity is correlated with its role in ASA recycling in the apoplast [112], and we observed lower ASA redox levels in the sensitive BHM-5 genotype (Table 3). A similar result was found by Billah et al. [113] in maize for DHAR and ASA activity.

The glyoxalase system consists of two enzymes, Gly I and Gly II, that convert the potential cytotoxic methylglyoxal (MG) to non-toxic hydroxy acids like lactate. Gly I uses GSH to convert MG to S-D-lactoyl glutathione (SLG), while Gly II catalyzes the hydrolytic reaction that liberates lactic acid and free GSH [114]. Upregulation or overexpression of these enzymes in several plant species has been shown to increase tolerance to abiotic stresses [50,59,115]. Our investigation revealed a higher accumulation of toxic MG in BHM-5, while a significantly lower accumulation was observed in the BIL214 × BIL218 genotype (Table 4) under salt stress conditions. Notably, the activities of Gly I and Gly II were statistically higher in the BIL214 × BIL218 genotype (Table 4), whereas BHM-5 displayed lower activity of these enzymes compared to other genotypes (Table 4). This suggests that high MG levels in BIL214 × BIL218 may be effectively converted to SLG, while lower Gly I and Gly II activities may have hindered MG detoxification and GSH recycling in BHM-5. These results highlight the contrast in stress tolerance and sensitivity between BIL214 × BIL218 and BHM-5. However, other genotypes like BHM-7 and BHM-9 showed significantly higher activity of Gly I but insignificant activity of Gly II (Table 4). Higher activities of Gly I and Gly II are directly linked to efficient MG detoxification and have been associated with effective stress tolerance in previous studies [51,57,115].

Correlation, heatmap analysis and PCA−biplot clearly shows that Na^+/K^+ levels are closely associated with NOX, ROS, and MG, falling into the same group (Figs. 3 and 4A, B). Redox homeostasis decreased with prolonged stress duration. The loss of CAT activity in sensitive genotypes on the 9th day of salt stress suggests that CAT activity induction may be critically important for long-term salt stress adaptation. On the other hand, GSTs are large multiple enzyme family with multiple function [96]. The increased GST activity can be associated with both growth and leaf senescence [116,117] which is agreement of our previous result [60]. Proline (Pro) is a low molecular amino acid that accumulates in plants in response to stress conditions with antioxidant and stomatal regulatory activity. In our study, Pro accumulated in maize, in both tolerant and sensitive genotypes, suggesting its role as a primary defense mechanism by maintaining osmotic pressure in cells [118]. The heatmap also demonstrates Pro accumulation under salt stress. Castañares et al. [119] demonstrated significant Pro accumulation in melon under salt stress.

5. Conclusions

In summary, our comprehensive analysis reveals that the sensitiveness of maize to salt stress is intricately linked to the regulation of Na^+/K^+ and ROS, which exhibits positive correlations with NOX activity. Furthermore, NOX-mediated generation of ROS and MG signaling pathways appear to be modulated under salt stress, potentially due to the overwhelming oxidative stress induced by elevated salt levels. The intricate interplay between NOX activity, ROS production, and antioxidant enzyme responses is contingent upon the salt sensitivity of the maize genotype under investigation. Our findings also highlight the importance of changes in isozyme patterns of antioxidant enzymes for ROS detoxification, reflecting redox alterations in specific cellular compartments. Notably, the induction of novel isozymes or the loss of existing ones suggests dynamic adjustments in response to salt-induced oxidative stress. While the relationship between NOX activity and MG detoxification remains to be fully elucidated as it requires NADPH-dependent GSH in presence of GR. In conclusion, this study underscores the multifaceted nature of maize's response to salt stress, shedding light on the intricate interactions between ion and redox homeostasis, ROS signaling, and antioxidant defenses. Further research is warranted to unravel the precise mechanisms governing these responses and to exploit this knowledge for the development of salt-tolerant maize varieties, contributing to global food security in the face of increasing environmental challenges. Moreover, the highly expressed CAT3, APX1 and APX2 isozymes intolerant genotypes under stress and recovery thrusted more research in biotechnological approach to improve salt tolerant maize variety.

Funding

We are grateful to the Ministry of Agriculture, Government of Bangladesh for funding this study.

Data availability statement

The datasets used and/or analyzed during the current study are available from the corresponding author on reasonable request.

CRediT authorship contribution statement

Md. Motiar Rohman: Writing – original draft, Methodology, Investigation, Formal analysis, Data curation, Conceptualization. **Md. Robyul Islam:** Writing – review & editing, Resources, Methodology, Formal analysis, Data curation. **Sheikh Hasna Habib:** Writing – review & editing, Validation, Resources, Investigation. **Dilwar Ahmed Choudhury:** Writing – review & editing, Software, Resources, Methodology. **Mohammed Mohi-Ud-Din:** Writing – review & editing, Visualization, Supervision, Software, Formal analysis.

Declaration of competing interest

The authors declare that they have no known competing financial interests or personal relationships that could have appeared to influence the work reported in this paper.

Acknowledgements

We acknowledge the supports provided by the Molecular Breeding Laboratory, BARI, Gazipur 1701, Bangladesh for carrying out this study.

Acronyms

APX	Ascorbate Peroxidase
ASA	Ascorbate (Vitamin C)
ATP	Adenosine Triphosphate
BHM-5	BARI Hybrid Maize 5
BHM-7	BARI Hybrid Maize 7
BHM-9	BARI Hybrid Maize 9
Ca	Calcium
Ca^{++}	Calcium Ions
CAT	Catalase
CO_2	Carbon Dioxide
CRD	Completely Randomized Design
DHA	Dehydroascorbate
DHAR	Dehydroascorbate Reductase
DNA	Deoxyribonucleic Acid
EDTA	Ethylenediaminetetraacetic Acid
Gly I	Glyoxalase I
Gly II	Glyoxalase II
GPX	Glutathione Peroxidase
GR	Glutathione Reductase
GSH	Reduced Glutathione
GSSG	Oxidized Glutathione
GST	Glutathione *S*-Transferase
H_2O	Water
H_2O_2	Hydrogen Peroxide
$HO^{\bullet}$	Hydroxyl Radical
K^{+}	Potassium
LOX	Lipoxygenase
MDA	Malondialdehyde
MDHAR	Monodehydroascorbate Reductase
Mg^{2+}	Magnesium Ions
N_2O	Nitrous Oxide
Na^{+}	Sodium Ions
NaCl	Sodium Chloride

NAD+ Nicotinamide Adenine Dinucleotide (oxidized form)
NADP+ Nicotinamide Adenine Dinucleotide Phosphate (oxidized form)
NADPH.Na_4 Sodium Salt of Nicotinamide Adenine Dinucleotide Phosphate (NADPH)
NADPH Nicotine Adenine Dinucleotide Phosphate
NH_3 Ammonia
NO Nitric Oxide
NOX NADPH Oxidase
O_2 Oxygen
$O_2^{\bullet-}$ Superoxide Anion Radical
Pb Lead
POD Peroxidase
RBOH Respiratory burst oxidase homolog
RNA Ribonucleic Acid
ROS Reactive Oxygen Species
ROS-Ca^{2+} hub Reactive Oxygen Species-Calcium Hub
SAS Statistical Analysis System
SE Standard Error
SOD Superoxide Dismutase
XTT 2,3-Bis−(2-Methoxy-4-Nitro-5-Sulfophenyl)−2H-Tetrazolium-5-Carboxanilide

Appendix A. Supplementary data

Supplementary data to this article can be found online at https://doi.org/10.1016/j.heliyon.2024.e26920.

References

[1] M. Muhammad, A. Waheed, A. Wahab, M. Majeed, M. Nazim, Y.H. Liu, L. Li, W.J. Li, Soil salinity and drought tolerance: an evaluation of plant growth, productivity, microbial diversity, and amelioration strategies, Plant Stress (2023) 100319, https://doi.org/10.1016/j.stress.2023.100319.
[2] T. Pan, M. Liu, V.D. Kreslavski, S.K. Zharmukhamedov, C. Nie, M. Yu, S. Shabala, Non-stomatal limitation of photosynthesis by soil salinity, Crit. Rev. Environ. Sci. Technol. 1–3551 (8) (2021) 791–825, https://doi.org/10.1080/10643389.2020.1735231.
[3] M.M. Liu, T. Pan, S.I. Allakhverdiev, M. Yu, S. Shabala, Crop halophytism: an environmentally sustainable solution for the global food security, Trends Plant Sci. 25 (7) (2020) 630–634, https://doi.org/10.1016/j.tplants.2020.04.008.
[4] M.M. Liu, H. Yu, B. Ouyang, C. Shi, V. Demidchik, Z. Hao, M. Yu, S. Shabala, NADPH oxidases and the evolution of plant salinity tolerance, Plant Cell Environ. 43 (2020) 2957–2968, https://doi.org/10.1111/pce.13907.
[5] M.S. Hossain, Present scenario of global salt-affected soils, its management and importance of salinity research, Int. Res. J. Biol. Sci. 1 (2019) 1–3.
[6] S. Shabala, J. Bose, R. Hedrich, Salt bladders: do they matter? Trends Plant Sci. 19 (11) (2014) 687–691, https://doi.org/10.1016/j.tplants.2014.09.001.
[7] M. Qadir, E. Quillérou, V. Nangia, G. Murtaza, M. Singh, R.J. Thomas, A.D. Noble, Economics of salt-induced land degradation and restoration, Nat. Resour. Forum 38 (4) (2014) 282–295, https://doi.org/10.1111/1477-8947.12054ff.
[8] R. Ozgur, B. Uzilday, A.H. Sekmen, I. Turkan, Reactive oxygen species regulation and antioxidant defense in halophytes, Funct. Plant Biol. 40 (9) (2013) 832–847, https://doi.org/10.1071/FP12389.
[9] V. Demidchik, Mechanisms of oxidative stress in plants: from classical chemistry to cell biology, Environ. Exp. Bot. 109 (2015) 212–228, https://doi.org/10.1016/j.envexpbot.2014.06.021.
[10] E.E. Farmer, M.J. Mueller, ROS-mediated lipid peroxidation and res-activated signaling, Annu. Rev. Plant Biol. 64 (2013) 429–450, https://doi.org/10.1146/annurev-arplant-050312-120132.
[11] M. Yoshioka-Nishimura, Close relationships between the PSII repair cycle and thylakoid membrane dynamics, Plant Cell Physiol. 57 (6) (2016) 1115–1122, https://doi.org/10.1093/pcp/pcw050.
[12] V. Raja, U. Majeed, H. Kang, K.I. Andrabi, R. John, Abiotic stress: interplay between ROS, hormones and MAPKs, Environ. Exp. Bot. 137 (2017) 142–157, https://doi.org/10.1016/j.envexpbot.2017.02.010.
[13] C. Zhao, H. Zhang, C. Song, J.K. Zhu, S. Shabala, Mechanisms of plant responses and adaptation to soil salinity, Innovation 1 (1) (2020), https://doi.org/10.1016/j.xinn.2020.100017.
[14] L. Novakovic, T. Guo, A. Bacic, A. Sampathkumar, K.L. Johnson, Hitting the wall-sensing and signaling pathways involved in plant cell wall remodeling in response to abiotic stress, Plants 7 (4) (2018) 89, https://doi.org/10.3390/plants7040089.
[15] M. Hasanuzzaman, H. Oku, K. Nahar, M.B. Bhuyan, J. Al Mahmud, F. Baluska, M. Fujita, Nitric oxide-induced salt stress tolerance in plants: ROS metabolism, signaling, and molecular interactions, Plant Biotechnol. Rep. 12 (2) (2018) 77–92, https://doi.org/10.1007/s11816-018-0480-0.
[16] J. Zhang, W. Liao, Protein S-nitrosylation in plant abiotic stresses, Funct. Plant Biol. 47 (1) (2020) 1–10, https://doi.org/10.1071/FP19071.
[17] J. Wang, R. Huang, Modulation of ethylene and ascorbic acid on reactive oxygen species scavenging in plant salt response, Front. Plant Sci. 10 (2019) 319, https://doi.org/10.3389/fpls.2019.00319.
[18] M. Kumar, M.S. Kesawat, A. Ali, S.-C. Lee, S.S. Gill, H.U. Kim, Integration of abscisic acid signaling with other signaling pathways in plant stress responses and development, Plants 8 (12) (2019) 592, https://doi.org/10.3390/plants8120592.
[19] J. Saha, E.K. Brauer, A. Sengupta, S.C. Popescu, K. Gupta, B. Gupta, Polyamines as redox homeostasis regulators during salt stress in plants, Front. Environ. Sci. 3 (2015) 21, https://doi.org/10.3389/fenvs.2015.00021.
[20] M.M. Julkowska, C. Testerink, Tuning plant signaling and growth to survive salt, Trends Plant Sci. 20 (9) (2015) 586–594, https://doi.org/10.1016/j.tplants.2015.06.008.
[21] P. Köster, L. Wallrad, K. Edel, M. Faisal, A. Alatar, J. Kudla, The battle of two ions: Ca^{2+} signaling against Na^{+} stress, Plant Biol. 21 (2019) 39–48, https://doi.org/10.1111/plb.12704.
[22] R.-J. Tang, C. Wang, K. Li, S. Luan, The CBL–CIPK calcium signaling network: unified paradigm from 20 years of discoveries, Trends Plant Sci. 25 (6) (2020) 604–617, https://doi.org/10.1016/j.tplants.2020.01.009.
[23] S. Shabala, Signalling by potassium: another second messenger to add to the list? J. Exp. Bot. 68 (15) (2017) 4003–4007, https://doi.org/10.1093/jxb/erx238.

[24] F. Rubio, M. Nieves-Cordones, T. Horie, S. Shabala, Doing 'business as usual' comes with a cost: evaluating the energy cost of maintaining plant intracellular K^+ homeostasis under saline conditions, New Phytol. 225 (3) (2020) 1097–1104, https://doi.org/10.1111/nph.15852.

[25] A.M. Ismail, T. Horie, Genomics, physiology, and molecular breeding approaches for improving salt tolerance, Annu. Rev. Plant Biol. 68 (2017) 405–434, https://doi.org/10.1146/annurev-arplant-042916-040936.

[26] R.L. Lopes-Marques, A.F. Nørrevang, P. Ache, A.T. Salvador, E.N. Van Loo, R. Hedrich, M. Palmgren, Prospects for accelerated domestication of the resilient plant quinoa, J. Exp. Bot. 71 (18) (2020) 5333–5347, https://doi.org/10.1093/jxb/eraa285.

[27] R. Munns, D.A. Day, W. Fricke, M. Watt, B. Arsova, B.J. Barkla, K.J. Foster, Energy costs of salt tolerance in crop plants, New Phytol. 225 (3) (2020) 1072–1090, https://doi.org/10.1111/nph.15864.

[28] C. Li, L.A. Mur, Q. Wang, X. Hou, C. Zhao, Z. Chen, J. Wu, Q. Guo, ROS scavenging and ion homeostasis is required for the adaptation of halophyte Karelinia caspia to high salinity, Front. Plant Sci. (13) (2022) 979956, https://doi.org/10.3389/fpls.2022.979956.

[29] N. Suzuki, S. Koussevitzky, R. Mittler, G. Miller, ROS and redox signaling in the response of plants to abiotic stress, Plant Cell Environ. 35 (2) (2012) 259–270, https://doi.org/10.1111/j.1365-3040.2011.02336.x.

[30] S. Gilroy, N. Suzuki, G. Miller, W.G. Choi, M. Toyota, A.R. Devireddy, R. Mittler, A tidal wave of signals: calcium and ROS at the forefront of rapid systemic signaling, Trends Plant Sci. 19 (10) (2014) 623–630, https://doi.org/10.1016/j.tplants.2014.06.013.

[31] V. Demidchik, S. Shabala, Mechanisms of cytosolic calcium elevation in plants: the role of ion channels, calcium extrusion systems and NADPH oxidase-mediated 'ROS-Ca^{2+} Hub, Funct. Plant Biol. 45 (2) (2018) 9–27, https://doi.org/10.1071/FP16420.

[32] C.H. Hu, P.Q. Wang, P.P. Zhang, X.M. Nie, B.B. Li, L. Tai, K.-M. Chen, NADPH Oxidases: the vital performers and center hubs during plant growth and signaling, Cell 9 (2) (2020) 437, https://doi.org/10.3390/cells9020437.

[33] J. Foreman, V. Demidchik, J.H. Bothwell, P. Mylona, H. Miedema, M.A. Torres, J.M. Davies, Reactive oxygen species produced by NADPH oxidase regulate plant cell growth, Nature 422 (6930) (2003) 442–446, https://doi.org/10.1038/nature01485.

[34] J.D. Lambeth, A.S. Neish, Nox enzymes and new thinking on reactive oxygen: a double-edged sword revisited, Annu. Rev. Pathol. 9 (2014) 119–145, https://doi.org/10.1146/annurev-pathol-012513-104651.

[35] J.S. Chung, J.K. Zhu, R.A. Bressan, P.M. Hasegawa, H. Shi, Reactive oxygen species mediate Na+-induced SOS1 mRNA stability in Arabidopsis, Plant J. 53 (3) (2008) 554–565, https://doi.org/10.1111/j.1365-313X.2007.03364.x.

[36] Y.J. Xie, S. Xu, B. Han, M.Z. Wu, X.X. Yuan, Y. Han, W.B. Shen, Evidence of Arabidopsis salt acclimation induced by upregulation of HY1 and the regulatory role of RbohD-derived reactive oxygen species synthesis, Plant J. 66 (2) (2011) 280–292, https://doi.org/10.1111/j.1365-313X.2011.04488.x.

[37] L. Ma, H. Zhang, L. Sun, Y. Jiao, G. Zhang, C. Miao, F. Hao, NADPH oxidase AtrbohD and AtrbohF function in ROS-dependent regulation of Na^+/K^+ homeostasis in Arabidopsis under salt stress, J. Exp. Bot. 63 (1) (2012) 305–317, https://doi.org/10.1093/jxb/err280.

[38] V. Demidchik, S.N. Shabala, K.B. Coutts, M.A. Tester, J.M. Davies, Free oxygen radicals regulate plasma membrane Ca^{2+}- and K^+-permeable channels in plant root cells, J. Cell Sci. 116 (2003) 81–88, https://doi.org/10.1242/jcs.00201.

[39] V. Demidchik, S. Shabala, S. Isayenkov, T.A. Cuin, I. Pottosin, Calcium transport across plant membranes: mechanisms and functions, New Phytol. 220 (1) (2018) 49–69, https://doi.org/10.1111/nph.15266.

[40] Y. Zhang, Y. Wang, J.L. Taylor, Z. Jiang, S. Zhang, F. Mei, J. Ni, Aequorin-based luminescence imaging reveals differential calcium signaling responses to salt and reactive oxygen species in rice roots, J. Exp. Bot. 66 (9) (2015) 2535–2545, https://doi.org/10.1093/jxb/erv043.

[41] T. Hu, K. Chen, L.X. Hu, E. Amombo, J.M. Fu, H_2O_2 and Ca^{2+}-based signaling and associated ion accumulation, antioxidant systems and secondary metabolism orchestrate the response to NaCl stress in perennial ryegrass, Sci. Rep. 6 (2016) 1–13, https://doi.org/10.1038/srep36396.

[42] M. Nath, D. Bhatt, A. Jain, S.C. Saxena, S.K. Saifi, S. Yadav, N. Tuteja, Salt stress triggers augmented levels of Na^+, Ca^{2+} and ROS and alter stress-responsive gene expression in roots of CBL9 and CIPK23 knockout mutants of *Arabidopsis thaliana*, Environ. Exp. Bot. 161 (2019) 265–276, https://doi.org/10.1016/j.envexpbot.2018.10.005.

[43] M. Zhu, M. Zhou, L. Shabala, S. Shabala, Physiological and molecular mechanisms mediating xylem Na^+ loading in barley in the context of salinity stress tolerance, Plant Cell Environ. 40 (7) (2017) 1009–1020, https://doi.org/10.1111/pce.12727.

[44] A. Martiniere, J.B. Fiche, M. Smokvarska, S. Mari, C. Alcon, X. Dumont, C. Maurel, Osmotic stress activates two reactive oxygen species pathways with distinct effects on protein nanodomains and diffusion, Plant Physiol. 179 (4) (2019) 1581–1593, https://doi.org/10.1104/pp.18.01065.

[45] M. Niu, Y. Huang, S. Sun, J. Sun, H. Cao, S. Shabala, Z. Bie, Root respiratory burst oxidase homologue-dependent H2O2 production confers salt tolerance on a grafted cucumber by controlling Na^+ exclusion and stomatal closure, J. Exp. Bot. 69 (14) (2018) 3465–3476, https://doi.org/10.1093/jxb/erx386.

[46] F. Hao, X. Wang, J. Chen, Involvement of plasma-membrane NADPH oxidase in nickel-induced oxidative stress in roots of wheat seedlings, Plant Sci. 170 (2006) 151–158, https://doi.org/10.1016/j.plantsci.2005.08.014.

[47] Y. Yang, S. Xu, L. An, N. Chen, NADPH oxidase-dependent hydrogen peroxide production, induced by salinity stress, may be involved in the regulation of total calcium in roots of wheat, J. Plant Physiol. 164 (2007) 1429–±1435, https://doi.org/10.1016/j.jplph.2006.08.009.

[48] M.A. Torres, J.L. Dangl, J.D.G. Jones, Arabidopsis gp91phox homologues AtrbohD and AtrbohF are required for accumulation of reactive oxygen intermediates in the plant defense response, Proc. Nat. Acad. Sci. U. S. A. 99 (2002) 517–522, https://doi.org/10.1073/pnas.012452499.

[49] Y. Zhang, B. Deng, Z. Li, Inhibition of NADPH oxidase increases defense enzyme activities and improves maize seed germination under Pb stress, Ecotoxicol. Environ. Saf. 158 (2018) 187–192, https://doi.org/10.1016/j.ecoenv.2018.04.028.

[50] M.A. Ahanger, C. Qin, N. Begum, M.Q. Maodong, X.X. Dong, M. El-Esawi, M.A. El-Sheikh, A.A. Alatar, L. Zhang, Nitrogen availability prevents oxidative effects of salinity on wheat growth and photosynthesis by up-regulating the antioxidants and osmolytes metabolism, and secondary metabolite accumulation, BMC Plant Biol. 19 (2019) 1–12, https://doi.org/10.1186/s12870-019-2085-3.

[51] K. Parvin, K. Nahar, M. Hasanuzzaman, M.B. Bhuyan, S.M. Mohsin, M. Fujita, Exogenous vanillic acid enhances salt tolerance of tomato: insight into plant antioxidant defense and glyoxalase systems, Plant Physiol. Biochem. 150 (2020) 109–120, https://doi.org/10.1016/j.plaphy.2020.02.030.

[52] A.A. Rodríguez, H.R. Lascano, D. Bustos, E. Taleisnik, Salinity-induced decrease in NADPH oxidase activity in the maize leaf blade elongation zone, J. Plant Physiol. 164 (3) (2007) 223–230, https://doi.org/10.1016/j.jplph.2006.07.014.

[53] Q. Wang, L. Ni, Z. Cui, J. Jiang, C. Chen, M. Jiang, The NADPH oxidase OsRbohA increases salt tolerance by modulating K^+ homeostasis in rice, Crop J. 10 (6) (2022) 1611–1622, https://doi.org/10.1016/j.cj.2022.03.004.

[54] B. Ijaz, E. Formentin, B. Ronci, V. Locato, E. Barizza, M.Z. Hyder, F. Lo Schiavo, T. Yasmin, Salt tolerance in indica rice cell cultures depends on a fine-tuning of ROS signaling and homeostasis, PLoS One 14 (4) (2019) e0213986, https://doi.org/10.1371/journal.pone.0213986.

[55] K. Kabała, M. Reda, A. Wdowikowska, M. Janicka, Role of plasma membrane NADPH oxidase in response to salt stress in cucumber seedlings, Antioxidants 11 (8) (2022) 1534, https://doi.org/10.3390/antiox11081534.

[56] Y. Sun, W. Liang, H. Cheng, H. Wang, D. Lv, W. Wang, M. Liang, C. Miao, NADPH Oxidase-derived ROS promote mitochondrial alkalization under salt stress in *Arabidopsis* root cells, Plant Signal. Behav. 16 (3) (2021) 1856546, https://doi.org/10.1080/15592324.2020.1856546.

[57] M.M. Rohman, M.Z.A. Talukder, M.G. Hossain, M.S. Uddin, M. Amiruzzaman, A. Biswas, A.F.M.S. Ahsan, M.A.Z. Chowdhury, Saline sensitivity leads to oxidative stress and increases the antioxidants in presence of proline and betaine in maize (*Zea mays* L.) inbred, Plant Omics J. 9 (1) (2016) 35–47.

[58] M.M. Rohman, S. Begum, M.Z.A. Talukder, A.H. Hossain, M.G. Uddin, M. Amiruzzaman, A.F.M.S. Ahsan, M.A.Z. Chowdhury, Drought sensitive maize inbred shows more oxidative damage and higher ROS scavenging enzymes, but no glyoxalases than a tolerant one at seedling stage, Plant Omics J. 9 (4) (2016) 220–232.

[59] S.A. Anjum, U. Ashraf, M. Tanveer, I. Khan, S. Hussain, B. Shahzad, A. Zohaib, F. Abbas, M.F. Saleem, I. Ali, Drought-induced changes in growth, osmolyte accumulation, and antioxidant metabolism of three maize hybrids, Front. Plant Sci. 8 (2017), https://doi.org/10.3389/fpls.2017.00069.

[60] M.M. Rohman, M.R. Islam, M.B. Monsur, M. Amiruzzaman, M. Fujita, M. Hasanuzzaman, Trehalose protects maize plants from salt stress and phosphorus deficiency, Plants 8 (12) (2019) 568, https://doi.org/10.3390/plants8120568.

[61] M.M. Rahman, M.G. Mostofa, M.A. Rahman, M.R. Islam, S.S. Keya, A.K. Das, M.G. Miah, A.R. Kawser, S.M. Ahsan, A. Hashem, B. Tabassum, Acetic acid: a cost-effective agent for mitigation of seawater-induced salt toxicity in mung bean, Sci. Rep. 9 (1) (2019) 1 5186, https://doi.org/10.1038/s41598-019-51178-w.

[62] M.M. Bradford, A rapid and sensitive method for the quantitation of microgram quantities of protein utilizing the principle of protein-dye binding, Anal. Biochem. 72 (1976) 248–254, https://doi.org/10.1006/abio.1976.9999.
[63] M.B. Monsur, N.A. Ivy, M.M. Haque, M. Hasanuzzaman, A. El Sabagh, M.M. Rohman, Oxidative stress tolerance mechanism in rice under salinity, Phyton 89 (3) (2020) 497, https://doi.org/10.32604/phyton.2020.09144.
[64] M. Jiang, J. Zhang, Water stress-induced abscisic acid accumulation triggers the increased generation of reactive oxygen species and up-regulates the activities of antioxidant enzymes in maize leaves, J. Exp. Bot. 53 (379) (2002) 2401–2410, https://doi.org/10.1093/jxb/erf090.
[65] U.K. Laemmli, Cleavage of structural proteins during the assembly of the head of bacteriophage T4, Nature 227 (1970) 680–685, https://doi.org/10.1038/227680a0.
[66] M. Sagi, R. Fluhr, Superoxide production by plant homologues of the gp91phox NADPH oxidase. Modulation of activity by calcium and by tobacco mosaic virus infection, Plant Physiol. 126 (3) (2001) 1281–1290, https://doi.org/10.1104/pp.126.3.1281.
[67] E.F. Elstner, A. Heupel, Inhibition of nitrite formation from hydroxyl ammonium chloride: a simple assay for superoxide dismutase, Anal. Biochem. 70 (1976) 616–620, https://doi.org/10.1016/0003-2697(76)90488-7.
[68] C.W. Yu, T.M. Murphy, C.H. Lin, Hydrogen peroxide-induced chilling tolerance in mung beans mediated through ABA independent glutathione accumulation, Funct. Plant Biol. 30 (2003) 955–963, https://doi.org/10.1071/FP03091.
[69] R.L. Heath, L. Packer, Photoperoxidation in isolated chloroplasts: I. Kinetics and stoichiometry of fatty acid peroxidation, Arch. Biochem. Biophys. 125 (1968) 189–198, https://doi.org/10.1016/0003-9861(68)90654-1.
[70] F. Chen, F. Wang, F. Wu, W. Mao, G. Zhang, M. Zhou, Modulation of exogenous glutathione in antioxidant defense system against Cd stress in the two barley genotypes differing in Cd tolerance, Plant Physiol. Biochem. 48 (2010) 663–672, https://doi.org/10.1016/j.plaphy.2010.05.001.
[71] H. Thordal-Christensen, Z. Zhang, Y. Wei, D.B. Collinge, Subcellular localization of H_2O_2 in plants, H_2O_2 accumulation in papillae and hypersensitive response during barley powdery mildew interaction, Plant J. 11 (1997) 1187–1194, https://doi.org/10.1046/j.1365-313X.1997.11061187.x.
[72] L.S. Bates, R.P. Waldren, I.D. Teare, Rapid determination of free proline for water-stress studies, Plant Soil 39 (1973) 205–207, https://doi.org/10.1007/BF00018060.
[73] T. Wei, V. Simko, R package "corrplot": visualization of a correlation matrix, Available online: https://github.com/taiyun/corrplot, 2017 (accessed on 29 September 2023).
[74] R. Kolde, pheatmap: Pretty Heatmaps, Version 1.0.12. rdrr.io 2019. Available online: https://rdrr.io/cran/pheatmap/(accessed on 29 September 2023)..
[75] S. Lê, J. Josse, F. Husson, FactoMineR: an R package for multivariate analysis, J. Stat. Software 25 (2008) 1–18, https://doi.org/10.18637/jss.v025.i01.
[76] H. Wickham, ggplot2: Elegant Graphics for Data Analysis, Springer, New York, NY, USA, 2016, https://doi.org/10.1007/978-3-319-24277-4_9.
[77] J.R. Acosta-Motos, M.F. Ortuño, A. Bernal-Vicente, P. Diaz-Vivancos, M.J. Sanchez-Blanco, J.A. Hernandez, Plant responses to salt stress: adaptive mechanisms, Agronomy 7 (2017) 18, https://doi.org/10.3390/agronomy7010018.
[78] M.M. Azooz, A.M. Ismail, M.A. Elhamd, Growth, lipid peroxidation and antioxidant enzyme activities as a selection criterion for the salt tolerance of maize cultivars grown under salinity stress, Int. J. Agric. Biol. 11 (1) (2009) 21–26.
[79] M.S. Kesawat, N. Satheesh, B.S. Kherawat, A. Kumar, H.U. Kim, S.M. Chung, M. Kumar, Regulation of reactive oxygen species during salt stress in plants and their crosstalk with other signaling molecules-Current perspectives and future directions, Plants 12 (4) (2023) 864, https://doi.org/10.3390/plants12040864.
[80] Y. Qu, M. Yan, Q. Zhang, Functional regulation of plant NADPH oxidase and its role in signaling, Plant Signal. Behav. 12 (8) (2017) e1356970, https://doi.org/10.1080/15592324.2017.1356970.
[81] J.D. Lambeth, NOX enzymes and the biology of reactive oxygen, Nat. Rev. Immunol. 4 (2004) 181–189, https://doi.org/10.1038/nri1312.
[82] E. Amicucci, K. Gaschler, NADPH oxidase genes from tomato (*Lycopersicon esculentum*) and curly-leaf pondweed (*Potamogeton crispus*), Plant Biol. 1 (1999) 524–528, https://doi.org/10.1055/s-2007-978547.
[83] H. Yoshioka, K. Sugie, H.J. Park, H. Maeda, N. Doke, Induction of plant gp91phoxhomolog by fungal cell wall, arachidonic acid, and salicylic acid in potato, Mol. Plant Microbe Interact. 14 (2001) 725–736.
[84] J.M. Kwak, I.C. Mori, Z.M. Pei, N. Leonhardt, M.A. Torres, J.L. Dangl, R.E. Bloom, S. Bodde, J.D. Jones, J.I. Schroeder, NADPH oxidase AtrbohD and AtrbohF genes function in ROS-dependent ABA signaling in *Arabidopsis*, EMBO J. 22 (2003) 2623–2633, https://doi.org/10.1094/MPMI.2001.14.6.725.
[85] H. Yoshioka, N. Numata, K. Nakajima, S. Katou, K. Kawakita, O. Rowland, J.D.G. Jones, N. Doke, *Nicotiana benthamiana* gp91phox homologs NbrbohA and NbrbohB participate in H_2O_2 accumulation and resistance to *phytophthora infestans*, Plant Cell 15 (2003) 706–718, https://doi.org/10.1105/tpc.008680.
[86] H. Wong, R. Pinontoan, K. Hayashi, R. Tabata, T. Yaeno, K. Hasegawa, C. Kojima, H. Yoshioka, K. Iba, T. Kawasaki, K. Shimamoto, Regulation of rice NADPH oxidase by binding of Rac GTPase to its N-terminal extension, Plant Cell 19 (2007) 4022–4034, https://doi.org/10.1105/tpc.107.055624.
[87] J. Nestler, S. Liu, T. Wen, A. Paschold, C. Marcon, H.M. Tang, F. Hochholdinger, Roothairless5, which functions in maize (*Zea mays* L.) root hair initiation and elongation, encodes a monocot-specific NADPH oxidase, Plant J. 79 (2014) 729–740, https://doi.org/10.1111/tpj.12578.
[88] K. Ben Rejeb, M. Benzarti, A. Debez, C. Bailly, A. Savouré, C. Abdelly, NADPH oxidase-dependent H2O2 production is required for salt-induced antioxidant defense in *Arabidopsis thaliana*, J. Plant Physiol. 174 (2015) 5–15, https://doi.org/10.1016/j.jplph.2014.08.022.
[89] K. Apel, H. Hirt, Reactive oxygen species: metabolism, oxidative stress, and signal transduction, Annu. Rev. Plant Biol. 55 (2004) 373–399, https://doi.org/10.1146/annurev.arplant.55.031903.141701.
[90] M. Janicka, M. Reda, K. Czyżewska, K. Kabała, Involvement of signaling molecules NO, H_2O_2 and H_2S in modification of plasma membrane proton pump in cucumber roots subjected to salt or low-temperature stress, Funct. Plant Biol. 45 (2018) 428–439, https://doi.org/10.1071/FP17095.
[91] R. Özgür Uzilday, B. Uzilday, T. Yalçinkaya, İ. Türkan, Mg deficiency changes the isoenzyme pattern of reactive oxygen species-related enzymes and regulates NADPH-oxidase-mediated ROS signaling in cotton, Turk. J. Biol. 41 (6) (2017) 868–880, https://doi.org/10.3906/biy-1704-39.
[92] R. Szőllősi, Superoxide dismutase (SOD) and abiotic stress tolerance in plants: an overview, Oxid. Damage Plants (2014) 89–129, https://doi.org/10.1016/B978-0-12-799963-0.00003-4.
[93] A. Sofo, A. Scopa, M. Nuzzaci, A. Vitti, Ascorbate peroxidase and catalase activities and their genetic regulation in plants subjected to drought and salinity stresses, Int. J. Mol. Sci. 16 (2015) 13561–13578, https://doi.org/10.3390/ijms160613561.
[94] L. Niu, W. Liao, Hydrogen peroxide signaling in plant development and abiotic responses: crosstalk with nitric oxide and calcium, Front. Plant Sci. 7 (2016) 230.
[95] K.J. Dietz, T. Pfannschmidt, Novel regulators in photosynthetic redox control of plant metabolism and gene expression, Plant Physiol. 155 (2011) 1477–1485, https://doi.org/10.3389/fpls.2016.00230.
[96] G. Noctor, L.A. Gomez, H. Vanacker, C.H. Foyer, Interactions between biosynthesis, compartmentation and transport in the control of glutathione homeostasis and signaling, J. Exp. Bot. 53 (372) (2002) 1283–1304, https://doi.org/10.1093/jexbot/53.372.1283.
[97] S. Shigeoka, T. Ishikawa, M. Tamoi, Y. Miyagawa, T. Takeda, Y. Yabuta, K. Yoshimura, Regulation and function of ascorbate peroxidase isoenzymes, J. Exp. Bot. 53 (2002) 1305–1319, https://doi.org/10.1093/jexbot/53.372.1305.
[98] L. Zhang, F. Chen, X. Zhang, Z. Li, Y. Zhao, R. Lohaus, X. Liu, The water lily genome and the early evolution of flowering plants, Nature 577 (7788) (2020) 79–84, https://doi.org/10.1038/s41586-019-1852-5.
[99] B. Jahan, M.F. AlAjmi, M.T. Rehman, N. Khan, Treatment of nitric oxide supplemented with nitrogen and sulfur regulate photosynthetic performance and stomatal behavior in mustard under salt stress, Physiol. Plantarum 168 (2020) 490–510, https://doi.org/10.1111/ppl.13056.
[100] M. Zeeshan, M. Lu, S. Sehar, P. Holford, F. Wu, Comparison of biochemical, anatomical, morphological, and physiological responses to salinity stress in wheat and barley genotypes deferring in salinity tolerance, Agronomy 10 (2020) 127, https://doi.org/10.3390/agronomy10010127.
[101] S.M. Alzahrani, I.A. Alaraidh, H. Migdadi, S. Alghamdi, M.A. Khan, P. Ahmad, Physiological, biochemical, and antioxidant properties of two genotypes of *Vicia faba* grown under salinity stress, Pakistan J. Bot. 51 (3) (2019) 786–798, https://doi.org/10.30848/PJB2019-3(3.
[102] S. Hiraga, K. Sasaki, H. Ito, Y. Ohashi, H. Matsui, A large family of class III plant peroxidases, Plant Cell Physiol. 42 (2001) 462–468, https://doi.org/10.1093/pcp/pce061.

[103] K. Asada, Ascorbate peroxidase: a hydrogen peroxide scavenging enzyme in plants, Physiol. Plantarum 85 (1992) 235–241, https://doi.org/10.1111/j.1399-3054.1992.tb04728.x.
[104] J.L. Jiang, Y. Tian, L. Li, M. Yu, R.-P. Hou, X.-M. Ren, H2S alleviates salinity stress in cucumber by maintaining the Na^+/K^+ balance and regulating H_2S metabolism and oxidative stress response, Front. Plant Sci. 10 (2019) 678, https://doi.org/10.3389/fpls.2019.00678.
[105] M.S. Attia, M.S. Osman, A.S. Mohamed, H.A. Mahgoub, M.O. Garada, E.S. Abdelmouty, A.A. Abdel Latef, Impact of foliar application of chitosan dissolved in different organic acids on isozymes, protein patterns, and physio-biochemical characteristics of tomato grown under salinity stress, Plants 10 (2) (2021) 388, https://doi.org/10.3390/plants10020388.
[106] C.H. Foyer, G. Noctor, Ascorbate and glutathione: the heart of the redox hub, Plant Physiol. 155 (2011) 2–18, https://doi.org/10.1104/pp.110.167569.
[107] R. Edwards, D.P. Dixon, Plant glutathione transferases, Methods Enzymol. 401 (2005) 169–186, https://doi.org/10.1016/S0076-6879(05)01011-6.
[108] Y. Nakano, K. Asada, Purification of ascorbate peroxidase in spinach chloroplasts; its inactivation in ascorbate-depleted medium and reactivation by monodehydroascorbate radical, Plant Cell Physiol. 28 (1) (1987) 131–140, https://doi.org/10.1093/oxfordjournals.pcp.a077268.
[109] A. Shalata, V. Mittova, M. Volokita, M. Guy, M. Tal, Response of the cultivated tomato and its wild salt-tolerant relative *Lycopersicon pennellii* to salt-dependent oxidative stress: the root antioxidative system, Physiol. Plantarum 112 (2001) 487–494, https://doi.org/10.1034/j.1399-3054.2001.1120405.x.
[110] E. Pinto, T.C. Sigaud-kutner, M.A. Leitao, O.K. Okamoto, D. Morse, P. Colepicolo, Heavy metal–induced oxidative stress in algae 1, J. Phycol. 39 (6) (2003) 1008–1018, https://doi.org/10.1111/j.0022-3646.2003.02-193.x.
[111] C. Miyake, K. Asada, Ferredoxin-dependent photoreduction of the monodehydroascorbate radical in spinach thylakoids, Plant Cell Physiol. 35 (4) (1994) 539–549, https://doi.org/10.1093/oxfordjournals.pcp.a078628.
[112] M.C. Rubio, P. Bustos-Sanmamed, M.R. Clemente, M. Becana, Effects of salt stress on the expression of antioxidant genes and proteins in the model legume *Lotus japonicus*, New Phytol. 181 (4) (2009) 851–859, https://doi.org/10.1111/j.1469-8137.2008.02718.x.
[113] M. Billah, M.M. Rohman, N. Hossain, M. Shalim Uddin, Exogenous ascorbic acid improved tolerance in maize (*Zea mays* L.) by increasing antioxidant activity under salinity stress, Afr. J. Agric. Res. 12 (17) (2017) 1437–1446.
[114] G. Noctor, A. Mhamdi, S. Chaouch, Y.I. Han, J. Neukermans, B.E.L.E.N. Marquez-Garcia, C.H. Foyer, Glutathione in plants: an integrated overview, Plant Cell Environ. 35 (2) (2012) 454–484, https://doi.org/10.1111/j.1365-3040.2011.02400.x.
[115] M. Hasanuzzaman, M.M. Alam, K. Nahar, S.M. Mohsin, M.B. Bhuyan, K. Parvin, B. Hawrylak-Nowak, M. Fujita, Silicon-induced antioxidant defense and methylglyoxal detoxification work coordinately in alleviating nickel toxicity in *Oryza sativa* L, Ecotoxicology 28 (2019) 261–276, https://doi.org/10.1007/s10646-019-02019-z.
[116] C. Chan, H.M. Lam, A putative lambda class glutathione S-transferase enhances plant survival under salinity stress, Plant Cell Physiol. 55 (3) (2014) 570–579, https://doi.org/10.1093/pcp/pct201.
[117] T. Kunieda, T. Fujiwara, T. Amano, Y. Shioi, Molecular cloning and characterization of a senescence-induced tau-class glutathione S-transferase from barley leaves, Plant Cell Physiol. 46 (9) (2005) 1540–1548, https://doi.org/10.1093/pcp/pci167.
[118] M. Turan, A.H. Elkarim, N. Taban, S. Taban, Effect of salt stress on growth, stomatal resistance, proline and chlorophyll concentrations on maize plant, Afr. J. Agric. Res. 4 (9) (2009) 893–897.
[119] J.L. Castañares, B. Corvalán, E.E. Larraburu, Effect of exogenous proline on physiological and growth traits of melon seedlings under salt stress, RIA: Rev. Investig. Agrop. 49 (2) (2023) 50–55, https://doi.org/10.58149/9e00-7x14.